Journal of Pain Research

Dovepress
Taylor & Francis Group

Open Access Full Text Article

ORIGINAL RESEARCH

Quantum Mechanical Mechanisms in the Therapeutic Effects of Spinal Cord Stimulation to Treat Chronic Neuropathic Pain: A Quantum Computational Model

Mahmoud Abdallat[1], Abdallah Barjas Qaswal[2], Ahmad Quzli[3], Moustafa Hassan[4], Sondos Alkhatib[3], Yazan Khraim[5], Ghufran Alkhateeb[6], Omar Alsmadi[7], Zaid Abdulqader[4], Jehad Shitawi[4], Hala Raed Miqdadi[2], Mariana Nuseir[8], Hussam IA Alzeerelhouseini[8], Sehrish Hanif[9], Omar Essa[10], Dima Yousef[10], Fatima Alsoub[10], Maram Okour[10], Ayham Alzubaidi[11], Omar Alsahli[12], Hasan El-Isa[13], Hussam Alsaddi[14], Mohamad Osama Al-Rashdan[2]

[1]Department of Neurosurgery, University of Jordan, Amman, 11942, Jordan; [2]Department of Psychiatry, Jordan University Hospital, Amman, 11942, Jordan; [3]West Suffolk NHS Foundation Trust, Suffolk, UK; [4]United Lincolnshire Hospital NHS Trust, Grantham, Lincolnshire, NG31 8JE, UK; [5]Hull University Teaching Hospital NHS Trust, Hull, HU3 2JZ, UK; [6]School of Medicine, University of Jordan, Amman, 11942, Jordan; [7]Colchester General Hospital, Colchester, CO4 5JL, UK; [8]Department of Internal Medicine, School of Medicine, University of Jordan, Amman, 11942, Jordan; [9]Bahria University, Islamabad, Islamabad Capital Territory, Pakistan; [10]Department of Family Medicine, School of Medicine, University of Jordan, Amman, 11942, Jordan; [11]School of Medicine, Jordan University of Science and Technology, Irbid, 22110, Jordan; [12]Alabdali Clemenceau Hospital, Amman, 11190, Jordan; [13]Jordanian Royal Medical Services, Amman, 11855, Jordan; [14]School of Medicine, Al-Baath University, Homs, Syria

Correspondence: Abdallah Barjas Qaswal, Email qaswalabdullah@gmail.com

Introduction: Spinal cord stimulation (SCS) is an emerging intervention used to treat neuropathic pain by inducing depolarization mediated by ion channels. According to the principles of classical electrophysiology, SCS will fail to induce depolarization if the barrier height of potassium channels is lower than that of sodium channels; moreover, the SCS seems to add more energetic burden on the neurons which may worsen the neuropathic pain. Therefore, our research question is "does quantum physics offer an alternative mechanism that may solve these two problematic concerns?".

Methods: In the present study, a mathematical model of quantum tunneling is applied on two-pore domain potassium channel K2P and sodium leak channel NALCN channels. The equations that describe the relationship between the external electric field produced from SCS and the membrane potential are stated clearly. Then, these equations are inserted in the MATLAB software to be solved for the membrane potential.

Results and discussion: Our results indicate that quantum tunneling model predicts the occurrence of depolarization induced by SCS even in the case that potassium channels have lower barrier height because the quantum model predicts that extracellular potassium ions have higher kinetic energy and higher tunneling probability compared to the intracellular potassium ions. As a result, net inward potassium current is generated and is able to depolarize the membrane potential. Hyperpolarization is predicted by the quantum model only in the case in which the influence of the external electric field on the kinetic energy of ions is considered and its direction is opposite to the direction of the electric field of the neuronal membrane. In addition, quantum tunneling-assisted depolarization utilizes lower energy compared to the depolarization induced by the classical opening of closed channels because the quantum tunneling of ions requires lower energy than the barrier height for the transport to occur.

Keywords: quantum tunneling, chronic pain, ion channels, spinal cord stimulation

Introduction

Chronic neuropathic pain is a common and disabling health problem.[1,2] Several etiologies lead to pain symptoms including diabetic neuropathy, post-herpetic neuralgia, trigeminal neuralgia, traumatic neuropathy, demyelinating diseases, chemotherapy-induced neuropathic pain, stroke, complex pain regional syndromes, fibromyalgia and many

https://doi.org/10.2147/JPR.S566042
Received: 21 September 2025
Accepted: 11 March 2026
Published: 1 April 2026

others.[3,4] Chronic neuropathic pain is characterized by peripheral and central sensitization due to hyper-excitability of neurons.[5] The hyperexcitability of neurons is attributed to three main mechanisms that include membrane depolarization, ectopic neuronal firing, and ephaptic coupling between neurons.[1,6–12] All these mechanisms lead to an increase in the pain signals coming from the periphery to the central brain regions.[1,6–12] The state of hyperexcitability of neurons results from the interaction of neurons, glia and immune cells to release various cytokines, chemokines, monoamines, and neuropeptides. In addition, the inflammation, trauma, ischemia and hypoxia affect the integrity of the neuronal membrane and their integral proteins including ion channels.[13] All these mediators and pathological changes alter the functions of several ion channels including sodium and potassium channels, which depolarize the membrane potential making neurons more excitable with a lower pain threshold.[14,15] Given the complexity of the chronic neuropathic pain, its treatment still poses a great challenge to physicians in the clinical practice even though several drugs are available including tricyclic antidepressants, serotonin-norepinephrine reuptake inhibitors (SNRIs), gabapentin, pregabalin and opioids such as tramadol and morphine.[16] Unfortunately, not all patients who are prescribed these analgesic agents achieve satisfactory outcomes; hence, other treatment modalities such as spinal cord stimulation (SCS) were introduced.[17]

SCS is a new emerging technique used to treat chronic pain by inserting electrodes in the epidural space that deliver electric impulses with certain frequency and amplitude, which elicit further excitation in the peripheral nerves.[17,18] This excitation generates antidromic and orthodromic action potentials that have segmental and supra-segmental therapeutic effects.[17,18] The basic mechanism of SCS seems paradoxical as the injured neurons implicated in the chronic pain show high levels of excitability. Therefore, researchers proposed several mechanisms of action that can explain the therapeutic effects of SCS. The gate theory, which is proposed by Ronald Melzack and Patrick Wall, states that activation of non-nociceptive fibers interferes with the pain signals via the antidromic action potentials.[17,18] In addition, orthodromic action potentials can activate supra-segmental anti-nociceptive pathways including noradrenergic and serotonergic neurons that have analgesic effects.[17,18] Furthermore, SCS can modulate the function of glial cells and the release of inflammatory mediators mitigating the inflammation that plays a role in maintaining pain.[17,18] Furthermore, the antidromic signals stimulate the segmental inhibitory neurons by releasing more GABA neurotransmitters.[17,18] Moreover, the stimulation provided by SCS via depolarization increases the release of other analgesic neurotransmitters such as endocannabinoids, acetylcholine and opioids.[17,18] In addition, SCS attenuates the activation of microglial cells which leads to the reduction in the release of the pro-inflammatory cytokines.[17,18] Interestingly, depolarization in the membrane of microglial cells is responsible for shifting these cells from the pro-inflammatory state to the ant-inflammatory state.[19,20] Therefore, the depolarization induced by SCS may represent the central mechanism that is responsible of the analgesic effects mediated by the chemical, electrical and cellular modulation.

There are several modes of nerve stimulation at the level of the spinal cord and these include Dorsal Root Ganglion-Stimulation (DRG-S), Paresthesia-Spinal Cord Stimulation (P-SCS) and paresthesia free-spinal cord stimulation (PF-SCS), which includes High Frequency-SCS (HF-SCS), Burst-SCS (B-SCS) and Evoked Compound Action potential-SCS.[18] The delivery of electric pulses by several methods of stimulation produces electric charges that distribute through the targeted area of the spinal cord. These charges induce electric fields (EFs) that can modulate the neuronal activity.[18] The amount of charge and thus the strength of the EF are related to the pulse width, the frequency of the pulses and the amplitude of the current.[18] P-SCS delivers a larger amount of charge that can produce a stronger EF if it is compared with PF-SCS. This explains the occurrence of paresthesia as a side effect of P-SCS due to the stronger EF that can elicit the generation of action potentials in A-beta neurons.[17,18] Therefore, EFs generated by PF-SCS are not strong enough to stimulate A-beta fibers; hence, the gate theory in this regard cannot explain the analgesic effects of PF-SCS.[17,18] P-SCS induces both orthodromic and antidromic action potentials that lead to segmental and supra-segmental mechanisms that result in pain relief; however, PF-SCS has not been shown to induce such analgesic mechanisms raising the quest to search for the specific mechanisms through which PF-SCS mediates the analgesic effects.[17,18] Reversible depolarization blockage and neuronal-glial modulation have been hypothesized as possible analgesic mechanisms of PF-SCS.[18]

The discussion of the mechanism of action of SCS is entirely based on the classical behavior of ions and their channels. However, an important aspect of ions' behavior needs to be addressed to complement our understanding of the mode of action of SCS, which is the quantum mechanical behavior of ions. Recently, it has been proposed that the

quantum behavior of sodium and potassium ions may contribute to the hyperexcitability in chronic neuropathic pain.[21] Focusing on the quantum phenomena within biological systems is a major aim of a new emerging field called quantum biology.[22] Quantum biology is a scientific area that represents the intersection between biology and quantum mechanics exploring the theoretical and experimental applicability of the principles of quantum mechanics on biological systems.[22] It provides quantum mechanical tools to investigate the quantum wave behavior of particles such as electrons, protons, ions and even molecules and their role in the biological processes.[22] One particular consequence of quantum mechanics, which will be implemented in this study, is quantum tunneling which is defined as a quantum transport of a particle through an energy barrier that its energy is higher than the energy of the particle. Quantum tunneling has been used to explain the mechanism of action of enzymes, the point DNA mutation and the transport of ions.[22] Moreover, several works provided evidence on the importance of the quantum effects in consciousness and neurotransmitter release in neurons.[23,24]

In the present study, we aim to extend the application of principles of quantum biology, particularly quantum tunneling, to provide a more comprehensive understanding of the mechanisms of SCS. Quantum tunneling transport implies that ions use energy less than the barrier height for the transport to occur,[22] while the classical transport implies that ions must have energy equals or higher than the barrier height for the transport to occur. On the other hand, quantum tunneling transport follows the rules of the quantum probability which is based on the Schrodinger equation and Max Born rule,[25] while the classical transport will be based on the principles of thermodynamics and Boltzmann distribution of energy. Besides, several mechanisms have been proposed to explain how the quantum behavior of particles such as ions can be sustained in the hot noisy biological environment.[26–31] These include environment-assisted quantum transport, the de-coherence-free subspace such as hydrophobic pockets and gates, the electromagnetic fields augmentation of the quantum fluctuations, the non-markovian dynamics and environmental memory, the quantum Zeno effect, topological protection and other mechanisms.[26–31]

If the electric fields produced by the SCS activate both sodium and potassium channels, then according to the classical electrophysiology, a depolarization is not expected to occur or even a hyperpolarization occur particularly at the resting state at which potassium ions have higher permeability, which comes in conflict with the basic mechanism of SCS. Moreover, inducing action potentials in neurons is an energy-consuming process from a classical point of view that puts neurons at the risk of ATP production failure, oxidative stress, inflammation, or even cell death which might worsen the neuropathic pain.[32–34] Hence, our research question is "does the quantum model provide more advantageous mechanisms that guarantee the occurrence of depolarization but with lower energetic burden on neurons?" Therefore, we aim to show that quantum tunneling of ions can explain the depolarization induced by the SCS in the resting state of neurons and with lower energy demand on them. Up to the authors' knowledge, this is the first study that explores the quantum mechanical aspects in the mechanism of spinal cord stimulation to treat chronic neuropathic pain by studying the influence of the electric field on the hydrophobic gate and its consequence on the quantum tunneling probability.

Materials and Methods

Several types of ion channels are involved in the pathophysiology of chronic neuropathic pain including two-pore domain potassium K2P channels and NALCN sodium channels.[35–38] In the present study, the mathematical model of the quantum tunneling of ions is applied to these ion channels which possess a hydrophobic gate[39,40] to explore and investigate the therapeutic effects of SCS. This model states that ions can behave wave-like while passing through the closed gates of ion channels. Specifically, ions can have a non-zero probability to pass through the closed gates via a quantum tunneling.[39,40] The quantum tunneling allows ions to pass through barriers whose potential energy is higher than the kinetic energy of ions, while the classical transport occurs only when the kinetic energy of ions is higher than the energy of the barrier. See Figure 1. Therefore, the tunneling of extracellular ions will be from the extracellular compartment to the intracellular one, while the intracellular ions tunnel from the intracellular compartment to the extracellular one.

Particularly, the two-pore domain potassium K2P channels and NALCN sodium channels block the passage of ions by posing an energy barrier made by hydrophobic amino-acids at the intracellular end.[41–46] However, the intracellular gate of K2P channel is formed by hydrophobic residues, while the intracellular gate of NALCN channel is not only

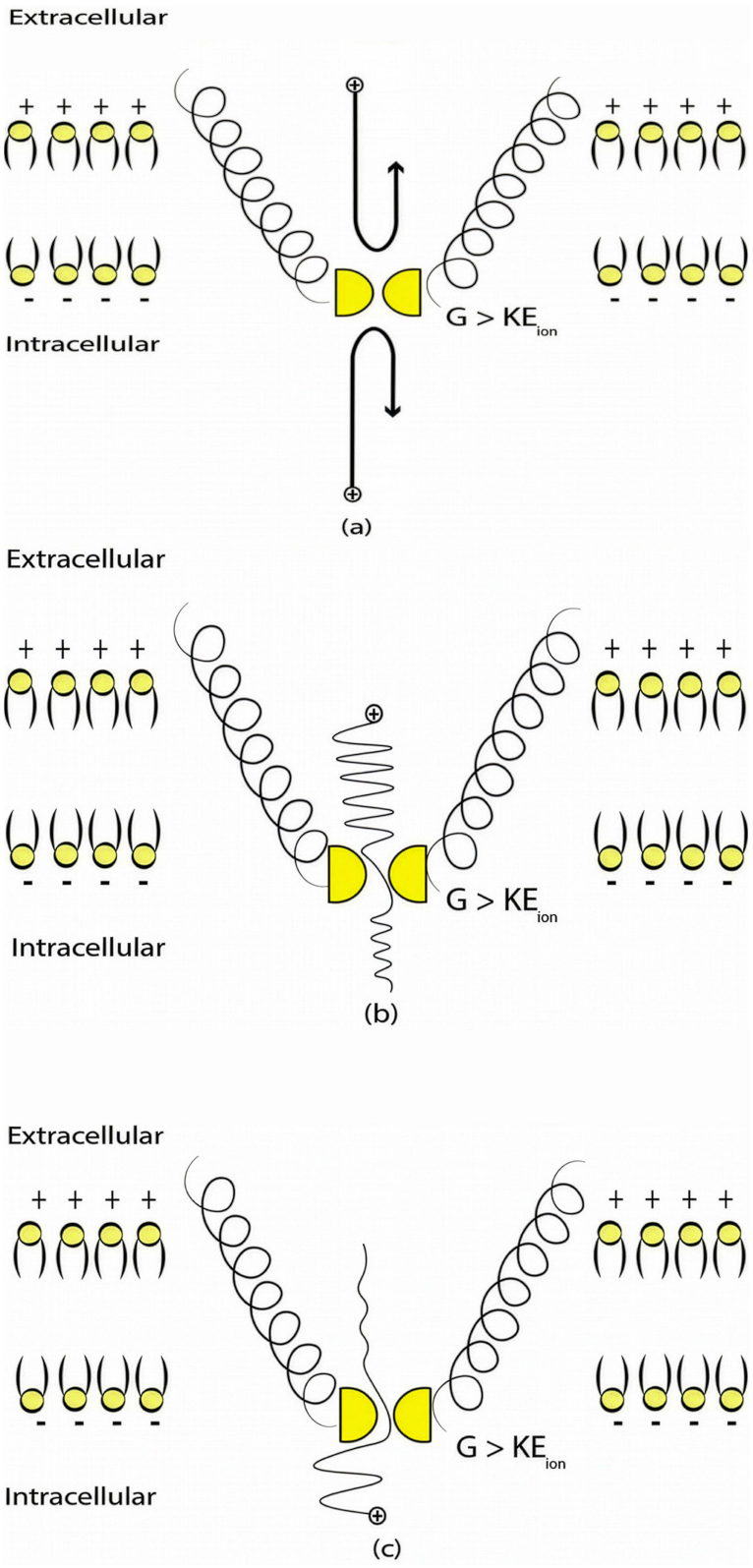

Figure 1 The figure represents a schematic illustration of the classical and quantum tunneling transports through the closed hydrophobic gate (shown in yellow) at the intracellular constriction of two alpha helices of an ion channel (two of them are shown for the sake of simplicity by the black helices) (**a**) In the classical transport, when the barrier height G is higher than the kinetic energy of the ion, the transport is not allowed because the energy requirement is not met, which is represented by the black reflected arrows. (**b**) In the quantum tunneling transport, when the barrier height is higher than the kinetic energy of extracellular ion, transport is allowed due to the quantum mechanical behavior of ions. (**c**) In the quantum tunneling transport, when the barrier height is higher than the kinetic energy of intracellular ions, transport is allowed due to the quantum mechanical behavior of ions. However, the tunneling probability of extracellular ions is higher than that of intracellular ion, which is represented by the higher wave amplitude for extracellular ions if it is compared with the wave amplitude of intracellular ions after passing the hydrophobic gate.

formed by hydrophobic residues but also by the hydrogen bonding between III–IV linker with II–III linker and S6 helix,[44–46] which indicates that the gate of NALCN channel is more tightly sealed off. See Figure 2. This discrepancy in the gating mechanism may explain why the resting conductance of potassium ions is higher than that of sodium ions, thus generating a potential that is negative inside with respect to the outside of the neuron.

These channels are also called leak channels that are responsible for the leaky conductance of potassium and sodium ions at the resting state of neurons. Hence, they are vital for establishing the neuron's resting membrane potential of – 70 mV. The negative sign indicates that it is negative inside with regard to the outside of the neuron. Therefore, these channels are suitable and reasonable molecular targets to study the influence of the electric field induced by SCS on the

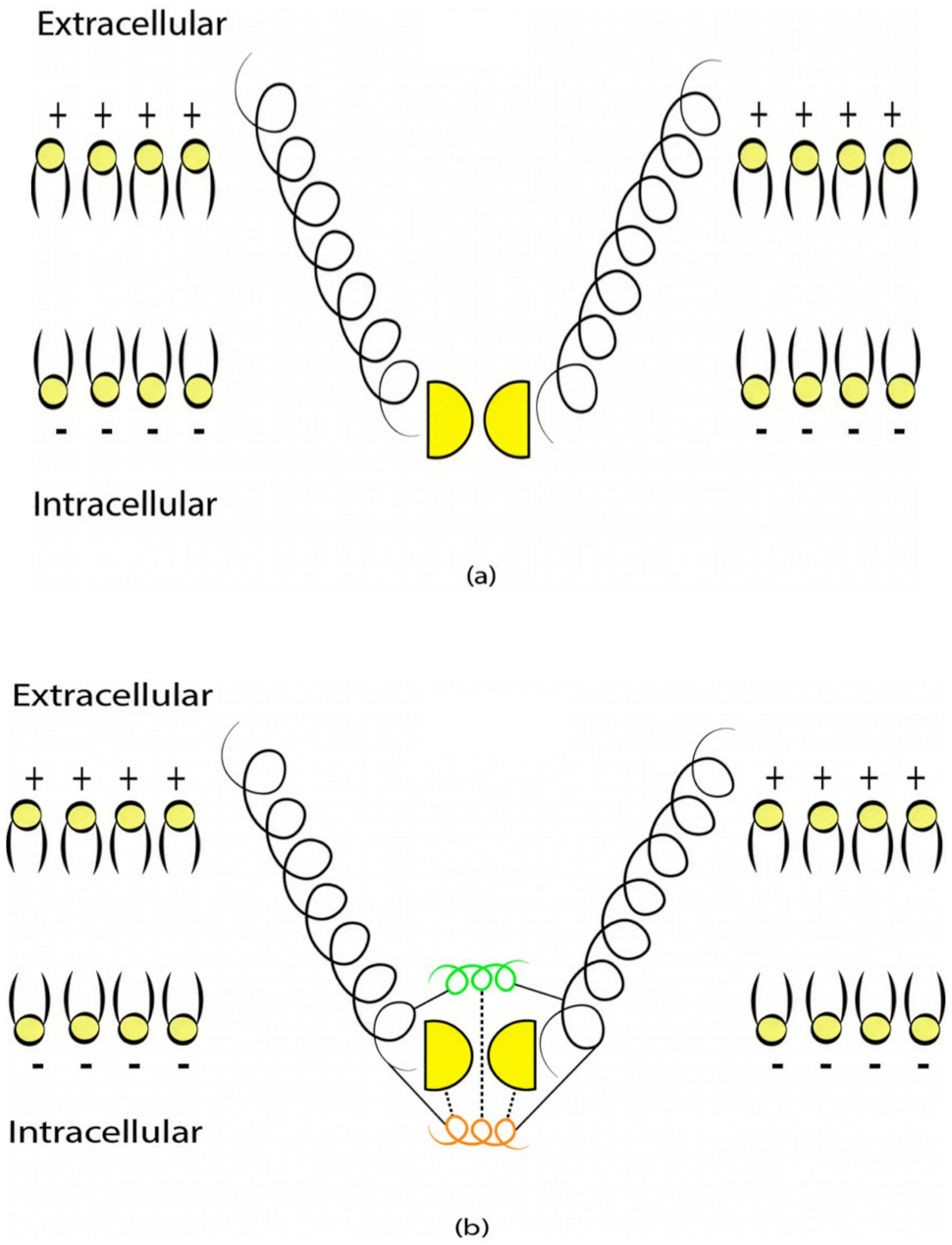

Figure 2 (**a**) A schematic representation of the intracellular gate of K2P channel which is sealed off by hydrophobic residues shown in yellow. (**b**) A schematic representation of the intracellular gate of NALCN channel which is not sealed off only by hydrophobic residues but also by a short alpha helix of III–IV linker (shown in Orange) which is stabilized by forming hydrogen bonds with the hydrophobic residues and another linker called II–III linker (shown in green). These channels are embedded within phospholipids (yellow heads with black tails as in the Figure) of the neuronal membrane. The potential of the membrane is negative (-) inside the neuron with respect to outside the neuron, which is positive (+).

https://doi.org/10.2147/JPR.S566042

excitability of neurons. Based on the studies using the potential mean forces (PMFs),[41–44,47] the shape of the hydrophobic barriers can be approximated using the symmetrical Eckart barrier, which can be given by the following equation:[48–50]

$$U(x) = \frac{G}{\cosh^2\left(\frac{x}{L}\right)} \tag{1}$$

where G is the barrier height, x is the position of the ion within the closed gate while passing through the barrier, and L is the barrier width at which $U(L) = 0.42G$. This equation tells us how difficult it is for ions to cross the closed gate at each point in terms of energetic cost. Thus, as U(x) value increases, it becomes harder for ions to cross that point and vice versa.

The symmetrical Eckart barrier can be represented as in Figure 3.

The symmetrical Eckart barrier is one of the widely used barriers to investigate the quantum tunneling probability of particles.[48–50] Particularly, the probability of quantum tunneling T_Q of ions through the symmetrical Eckart barrier can be calculated by the following equation:[48–50]

$$T_Q = e^{-\alpha L\left(\sqrt{G}-\sqrt{KE}\right)}, \tag{2}$$

where $\alpha = \frac{\sqrt{8\pi^2 M}}{\hbar}$ in which M is the mass of the ion and $\hbar$ is the reduced Planck constant and KE is the kinetic energy of the ion.Based on equation (2), four physical factors can determine the value of tunneling probability T_Q. These include the mass of the ion, the length of the barrier, the barrier height and the kinetic energy of the ion. The relationship between T_Q and the four physical factors is exponential and is represented by the base of e, the Euler's number, which is approximated by the value of 2.718. This means that the value of T_Q is very sensitive to changes in the four physical factors. As the values of gate length, the mass of ion and the barrier height increase, the tunneling probability decreases and vice versa, while as the kinetic energy of the ion increases, the tunneling probability increases.

The kinetic energy of ions varies according to their compartments. Since the closed gate is located at the intracellular end (See Figure 2), the extracellular ions while passing through the neuronal membrane acquire kinetic energy because the electric potential of the membrane is negative inside with regard to outside, while intracellular ions hit the gate before going through the membrane potential. See Figure 1. Therefore, the kinetic energy of extracellular ions KE_o and intracellular ions KE_i can be calculated by the following equations, respectively:

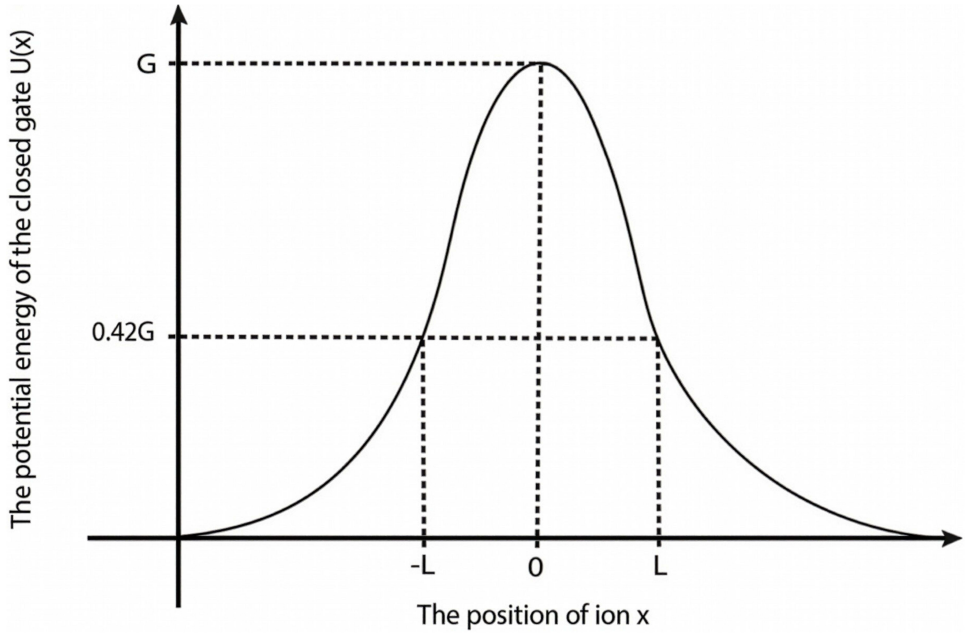

Figure 3 A schematic diagram that illustrates the potential energy of the closed gate U(x), the position of the ions within the hydrophobic gate x, the barrier height G and the length of the gate L at which U(x) = 0.42 G.

$$KE_o = qV_m + \frac{1}{2}K_BT, \tag{3}$$

$$KE_i = \frac{1}{2}K_BT, \tag{4}$$

where q is the charge of ion, V_m is the neuron's membrane potential, and $\frac{1}{2}K_BT$ is the average thermal kinetic energy of ions in which K_B is the Boltzmann constant and T is the absolute body temperature in the unit of Kelvin (K). Here, $\frac{1}{2}K_BT$ is used instead of $\frac{3}{2}K_BT$ because ions are moving in one dimension (1D). The influence of the internal electric field on the kinetic energy of intracellular ions is not considered in Equation (4) because the length of the gate is small compared to the thickness of the membrane making the contribution of the internal electric field to the kinetic energy of intracellular ions small compared to extracellular ions yielding negligible impact on the values of the membrane potential since the tunneling probability is exponentially sensitive to the kinetic energy of the ions. Therefore, we neglect the influence of the internal electric field on the intracellular ions to make the framework simple without affecting the numerical results and their corresponding conclusions. Based on Equations (3) and (4), the extracellular ions are expected to have higher kinetic energy and thus higher tunneling probability if they are compared with the intracellular ions. See Figure 1.

The external electric fields produced from SCS induce wetting in the hydrophobic gate of channels.[51] This wetting decreases the energy barrier of the gate making the passage of ions more permitted. This effect is demonstrated in serotonin receptor-3 (5-HT3) receptor, which possesses a hydrophobic gate, under the influence of an external field.[51] K2P and NALCN channels also have a hydrophobic gate and thus they are candidate targets to be influenced by SCS. Interestingly, both directions of electric field (the same and the opposite of the direction of the internal electric field of neuronal membrane) can hydrate the hydrophobic pore and increase the permeability of ions.[51] However, the one with the same direction of the electric field of neuronal membrane induces wetting with a higher probability of hydration.[51] See Figure 4.

The influence of the external electric field on the barrier height of the gate can be evaluated by the following equation:[51]

$$G^* = G - m(E - E_{INT})^2, \tag{5}$$

where G^* is the decreased barrier height under the influence of the external electric field, m refers to the strength of the coupling between hydration probability and the strength of the external electric field with a unit of ($10^{-20}\times$ J.m^2.V^{-2}), so this factor quantifies the extent to which the electric field lowers the energy barrier, thus facilitating ion entry through the gate, E is the external electric field induced by SCS, and E_{INT} is the intrinsic electric field arising from the charged amino acids of the channel protein,[51] which counteracts the electric field induced by SCS. According to this equation, three physical factors contribute to the magnitude of the decrease in the barrier height of the closed gate. As the coupling factor m and the external electric field E increase, the drop in the barrier height increases, and thus the hydration probability increases, while as the intrinsic electric field increases, it becomes more difficult for the external electric field to decrease the barrier height and to increase the hydration probability.

Based on equation (5), the differential effect of the direction of the external electric field can be explained by m values. The external electric field with the direction of the internal electric field of the neuronal membrane may have higher m value compared with the electric field with the opposite direction. Hence, it has higher coupling between hydration probability and the strength of the electric field.[45] In both cases, the electric field reduces the barrier height of the gate by the magnitude of $m(E - E_{INT})^2$. See Figure 5.

In this study,[52] the focus was the influence of the external electric fields on the selectivity filter of voltage-gated channels, which is different from our molecular target studied in our work. In the same study,[52] the external electric fields increase the rigidity of the selectivity filter, which is made by several carbonyl oxygens. The increase in the rigidity is attributed to the decrease in the radius of the selectivity filter. As a consequence, the depth of the energy barrier increases and the flow of ions decreases. However, in our work, we focused on the influence of the electric fields on the energetics of the hydrophobic gate of the major leaky channels, which do not have selectivity filter. Our work is based on the idea that the external electric field can decrease the barrier heights of the hydrophobic gate, which is the opposite outcome

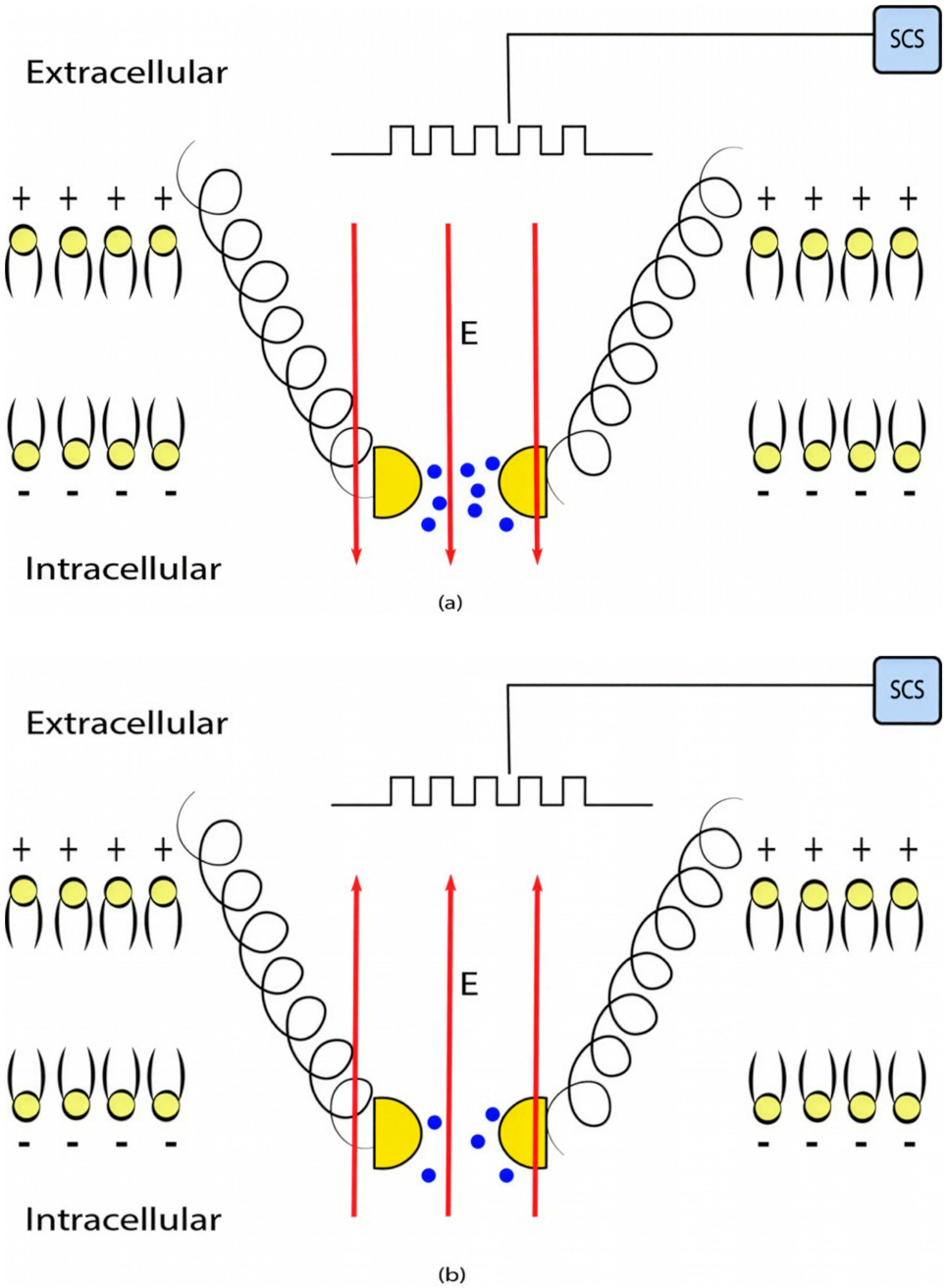

Figure 4 The figure represents a schematic representation of wetting (hydrating) the hydrophobic pore under the influence of the external electric field. The probability of hydration is higher when the direction of the external electric field goes with the direction of the electric field of the neuronal membrane as in (**a**) compared when it is in opposite direction as in (**b**). The figure shows two conditions for the angle between the electric field and membrane potential, which are 0 and 180 in (a) and (b) respectively. The effect when the angle is between them needs to be verified by experimental studies. The blue dots refer to water molecules and their number indicates the hydration probability. The higher is the number of the blue dots, the higher is the hydration probability. The external electric field is represented by the red arrows and the electrical pulses by the black stepwise lines.

found in the selectivity filter. The difference in the final outcome is related to the changes in the molecular structures between the selectivity filter and the hydrophobic gate; hence, the interaction with the external electric field will be different. The external electric field increases wetting (hydration) within hydrophobic particles.[53] This statement was supported because the external electric fields decrease the thickness of the hydrophobic layer near hydrophobic particles weakening the adsorption between the hydrophobic particles and the gas molecules and making the H_2O molecules more mobile. The thinning hydrophobic layer means that the range of hydrophobic attraction becomes small, which is

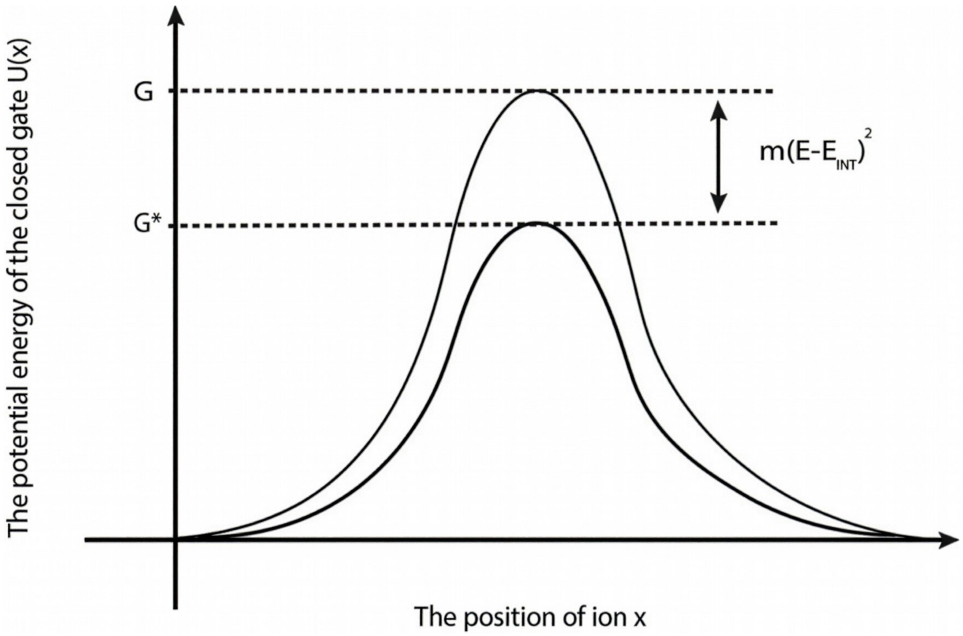

Figure 5 The figure represents a schematic diagram that illustrates the drop in the barrier height of the hydrophobic gate under the influence of the electric field. The drop in the barrier height is by the magnitude of $m(E - E_{INT})^2$.

disadvantageous for the adhesion of the dissolved gas on the hydrophobic surface.[53] The accumulative evidence indicates that dewetting (dehydration) increases the energy burden on ion passage while wetting decreases the barrier energy by adopting the aqueous state which facilitates the passage of ions.[42,54]

The influence of the external electric field on the kinetic energy of ions can be calculated according to two conditions:

1) when the direction of the external electric field is with the direction of the electric field of the neuronal membrane and in this case the kinetic energy of ions can be investigated according to these equations:

$$KE_o = qV_m + \frac{1}{2}K_BT + Edq, \tag{6}$$

Equation (6) refers to the kinetic energy of extracellular ions under the influence of the external electric field and the internal electric field of the neuronal membrane.

On the other hand, the influence made by the external electric field on the intracellular ions can be calculated by this mathematical expression $KE_i = \frac{\frac{1}{2}K_BT + \frac{1}{K_BT}\int_{ELq}^{\infty}(Z-ELq)e^{\frac{-Z}{K_BT}}dZ}{2}$. However, when we solve the integral $\frac{1}{K_BT}\int_{ELq}^{\infty}(Z - ELq)e^{\frac{-Z}{K_BT}}dZ$ using MATLAB, it will be reduced to $K_BTe^{\frac{-ELq}{K_BT}}$, and the mathematical expression becomes:

$$KE_i = \frac{\frac{1}{2}K_BT + K_BTe^{\frac{-ELq}{K_BT}}}{2}, \tag{7}$$

where Z is the thermal energy, d is the thickness of the neuronal membrane, q is the charge of the ion, and L is the length of the gate. The thermal energy Z refers to all possible values of kinetic energy at certain body temperature and $\frac{1}{2}K_BT$ is the average value of all these values. In equation (7), the kinetic energy of the intracellular ion is calculated as the average of the two values at the beginning and the end of the gate.

2) When the direction of the external electric field is the opposite of the direction of the electric field of the neuronal membrane and in this case the kinetic energy of ions can be calculated by the following equations:

https://doi.org/10.2147/JPR.S566042

$$KE_o = qV_m + \frac{1}{2}K_BT - Edq, \tag{8}$$

$$KE_i = \frac{1}{2}K_BT + \frac{ELq}{2}, \tag{9}$$

In equation (9), the kinetic energy of the intracellular ion is calculated as the average of the two values at the beginning and the end of the gate. At the beginning of the gate, the kinetic energy of intracellular ions is $\frac{1}{2}K_BT$ and at the end of the gate, their kinetic energy is $\frac{1}{2}K_BT + ELq$. Taking the average of these two expressions, this gives Equation (9).

The term qV_m reflects the influence of the internal electric field of the neuronal membrane on the kinetic energy of ions, while the term Edq or ELq reflects the influence of the external electric field on kinetic energy of ions.

In our paper, we are going to investigate the relationship between the external electric field and the membrane potential when the effect of the external electric field on the kinetic energy of ions is not considered in the calculations and then when this effect is considered in the calculations. The former case occurs when the external electric field is applied for a sufficiently long time than the time required to reach a new steady state for the neuronal membrane potential, while the latter case occurs when the external electric field is applied for a time shorter than the time required to reach the new steady state. We will address both cases to provide more comprehensive understanding of the quantum mechanical mechanisms of the SCS.

The quantum tunneling of ions through the closed ion channels results in quantum flow of ions, which can be quantified by the quantum conductance. The quantum unitary conductance C_q of ions of single channel can be calculated by the following equation:[50]

$$C_Q = \frac{q^2}{h}T_Q, \tag{10}$$

where h is the Planck constant, q is the charge of the ion and T_Q is the tunneling probability. The unit of C_Q will be Siemens (S). The quantum unitary conductance tells us how permeable this channel is to a particular ion via quantum tunneling. The quantum membrane conductance MC_Q due to quantum tunneling in a certain number of ion channels can be calculated by the following equation:[55]

$$MC_Q = C_Q \times D, \tag{11}$$

where D is the density of ion channels within the membrane with a unit of m^{-2}. Thus, the unit of the quantum membrane conductance is $S.m^{-2}$. The quantum membrane conductance tells us how permeable the membrane is to a particular ion via quantum tunneling.

Moreover, the quantum unitary conductance and the quantum membrane conductance depend on the value of tunneling probability, thus they will be very sensitive to the changes in the length of the barrier, the mass of the ion, the barrier height, and the kinetic energy of the ion as we explained before.

To evaluate the interplay between the quantum tunneling probability, the strength of the electric field and the resting membrane potential of neurons, the quantum version of the Goldman-Hodgkin-Katz (GHK) equation can be used:[56]

$$[Na]_o\left(MC_{Na} + MC_{Q-Na(o)}\right) + [K]_o\left(MC_K + MC_{Q-K(o)}\right) = e^{\frac{-qV_m}{K_BT}}\left(([Na]_i\left(MC_{Na} + MC_{Q-Na(i)}\right) + [K]_i\left(MC_K + MC_{Q-K(i)}\right)\right), \tag{12}$$

where $[Na]_o$ is the extracellular concentration of sodium ions, $[K]_o$ is the extracellular concentration of potassium ions, $[Na]_i$ is the intracellular concentration of sodium ions, $[K]_i$ is the intracellular concentration of potassium ions, MC_{Na} is the leaky membrane conductance of sodium ions, MC_K is the leaky membrane conductance of potassium ions, $MC_{Q-Na(o)}$ is the quantum membrane conductance of extracellular sodium ions, $MC_{Q-K(o)}$ is the quantum membrane conductance of extracellular potassium ions, $MC_{Q-Na(i)}$ is the quantum membrane conductance of intracellular sodium ions, $MC_{Q-K(i)}$ is the quantum membrane conductance of intracellular potassium ions, V_m is the resting membrane potential, K_B is the Boltzmann constant, and T is the absolute body temperature in the unit of Kelvin (K). The standard form of the GHK equation contains one value of conductance for potassium and sodium ions. However, since quantum conductance is

introduced and is calculated by different equations from the classical (leaky) conductance, we modified the equation so that the total conductance is the sum of the classical and quantum conductance values.

On the other hand, the influence of the electric fields induced by SCS on the classical transport of ions through open channels and its relation to the resting membrane potential can be assessed by the following equation:[55]

$$[Na]_o\left(MC_{Na}+D_{Na}C_{Na}\frac{1}{1+e^{\frac{G^*}{K_BT}}}\right)+[K]_o\left(MC_K+D_KC_K\frac{1}{1+e^{\frac{G^*}{K_BT}}}\right)$$
$$=e^{\frac{-qV_m}{K_BT}}\left([Na]_i(MC_{Na}+D_{Na}C_{Na}\frac{1}{1+e^{\frac{G^*}{K_BT}}}\right)+[K]_i\left(MC_K+D_KC_K\frac{1}{1+e^{\frac{G^*}{K_BT}}}\right), \quad (13)$$

where C_{Na} is the unitary conductance of the sodium channel when it is open and C_K is the unitary conductance of the potassium channel when it is open. A value of 1×10^{-12} S will be used for both sodium and potassium channels.[50] Equation (13) is similar to equation (12) except that we evaluate the effect of the drop in the barrier height on the classical conductance of potassium and sodium channels based on the Boltzmann distribution of the thermal energy and thus the effect on the resting membrane potential. In other words, we evaluate the ability of the thermal biological environment to affect the classical conductance in response to the drop in the barrier height by providing sufficient energy to open the closed channels.

Results

In this section, we are going to explore the relationship between the strength of the external electric field produced by SCS and the neuron's membrane potential according to the quantum and classical transports. This will enable us to reveal the quantum mechanical aspects of the therapeutic effects of SCS to treat chronic neuropathic pain. Six different values of *m* are used to study the quantum mechanical aspects of SCS, which are 200, 210,220, 300, 310, and 320 based on the results obtained in this reference.[51] According to this reference, the m parameter takes a wide range of values depending on the water model and the level of pore hydration, hence we choose several values to capture the wide range and provide a comprehensive understanding of the influence of the m parameter on quantum tunneling. These values have the unit of 10^{-20} J nm^2 V^{-2}. Moreover, E_{INT} values take the range between (1–2) $\times10^7$ V/m according to the same reference, which will be considered in the following analyses. In addition, we will use the values of the physical parameters described in the previous section, which can be found in Table 1. The values of the constants in the table above are universal and have been used in the biological environment of neurons.[55] The values of ions concentrations and their conductance have been validated and used across many physiological studies and are applicable to neurons. They are set to yield a neuronal

Table 1 The Values of the Physical Parameters Used in the Present Study

Parameter	Value
The thickness of neuronal membrane d	7×10^{-9} m
The length of the closed gate L	1×10^{-9} m
The mass of sodium	3.8×10^{-26} Kg
The mass of potassium	6.5×10^{-26} Kg
Extracellular sodium concentration $[Na]_o$	142 mmol/L
Intracellular sodium concentration $[Na]_i$	14 mmol/L
Extracellular potassium concentration $[K]_o$	4 mmol/L
Intracellular potassium concentration $[K]_i$	140 mmol/L
The charge of sodium ion	1.6×10^{-19} C

(*Continued*)

https://doi.org/10.2147/JPR.S566042

Table 1 (Continued).

Parameter	Value
The charge of potassium ion	1.6×10^{-19} C
The leaky membrane conductance of sodium MC_{Na}	0.22 S/m^2
The leaky membrane conductance of potassium MC_K	5 S/m^2
The Planck constant h	6.6×10^{-34} Js
The reduced Planck constant $\hbar$	1.05×10^{-34} Js
The Boltzmann constant K_B	1.38×10^{-23} J/K
The Body temperature T	310 K
The gas constant R	8.314 J/mol.K
The Faraday's constant F	96485 C/mol
The density of channels D	100 channels per μm^2

membrane potential of 0.07 V,[55] which will be used as a reference point to observe any depolarization or hyperpolarization. The length of the closed gate ranges between several angstroms up to one nanometer, hence we chose one nanometer as the maximum value because it would be more feasible to apply the conclusions on the lower values since the quantum behavior and quantum tunneling is more evident on the smaller scale.[41]

Using MATLAB software, all the equations described in the previous section are inserted in the software and the values presented in the above mentioned table are substituted. The software will solve Equation (12) for the dependent variable, the membrane potential Vm, with respect to the intensity of the external electric field E that is expected to alter the potential at different values of m, G and E_{INT}. Then, the relationship between the membrane potential and electric field is plotted. The plots obtained will represent the influence of the external electric field on the membrane potential mediated by the quantum tunneling through the closed gate. The same methodological approach will be applied on Equation (13) to obtain the plots for the classical model. To ensure computational accuracy, the steady state of the net flow of ions for both classical and quantum models is found by solving the GHK equation as an implicit function using the MATLAB fimplicit function and tracing its zero-contour. In addition, we used the parameter MeshDensity to be 500 to get high-resolution trace of the zero-level curve of GHK equations.

The influence of the electric field induced by SCS on the neuron's membrane potential according to the quantum tunneling transport without considering its influence on the kinetic energy of ions

Because the external electric field will affect both potassium and sodium channels, it is important to assess the relationship between the strength of the electric field and the neuron's membrane potential under the influence of the quantum tunneling of both potassium and sodium ions together. Figure 6 will assess such relationship when the barrier height $G_{Na,K} = 5 \times 10^{-20}$ J and $G_{Na,K} = 10 \times 10^{-20}$ J[41–44] based on Equation (12).

We are interested in investigating the situation in which the barrier height of the closed gate of potassium channels is lower than that of sodium channels. This assumption is rationalized because the leaky membrane conductance of potassium ions is higher than that of sodium ions and the closed gate of potassium K2P channels is less strictly sealed off if they are compared with NALCN channels as we explained before. We will study two cases:

1. $G_K = 5 \times 10^{-20}$ J and $G_{Na} = 10 \times 10^{-20}$ J and,
2. $G_K = 8 \times 10^{-20}$ J and $G_{Na} = 10 \times 10^{-20}$ J.

The relationship between the strength of the electric field and the neuron's membrane potential under the influence of the quantum tunneling of both potassium and sodium ions according to the both cases can be investigated. See Figure 7.

The influence of the electric field induced by SCS on the neuron's membrane potential according to the quantum tunneling transport considering its influence on the kinetic energy of ions

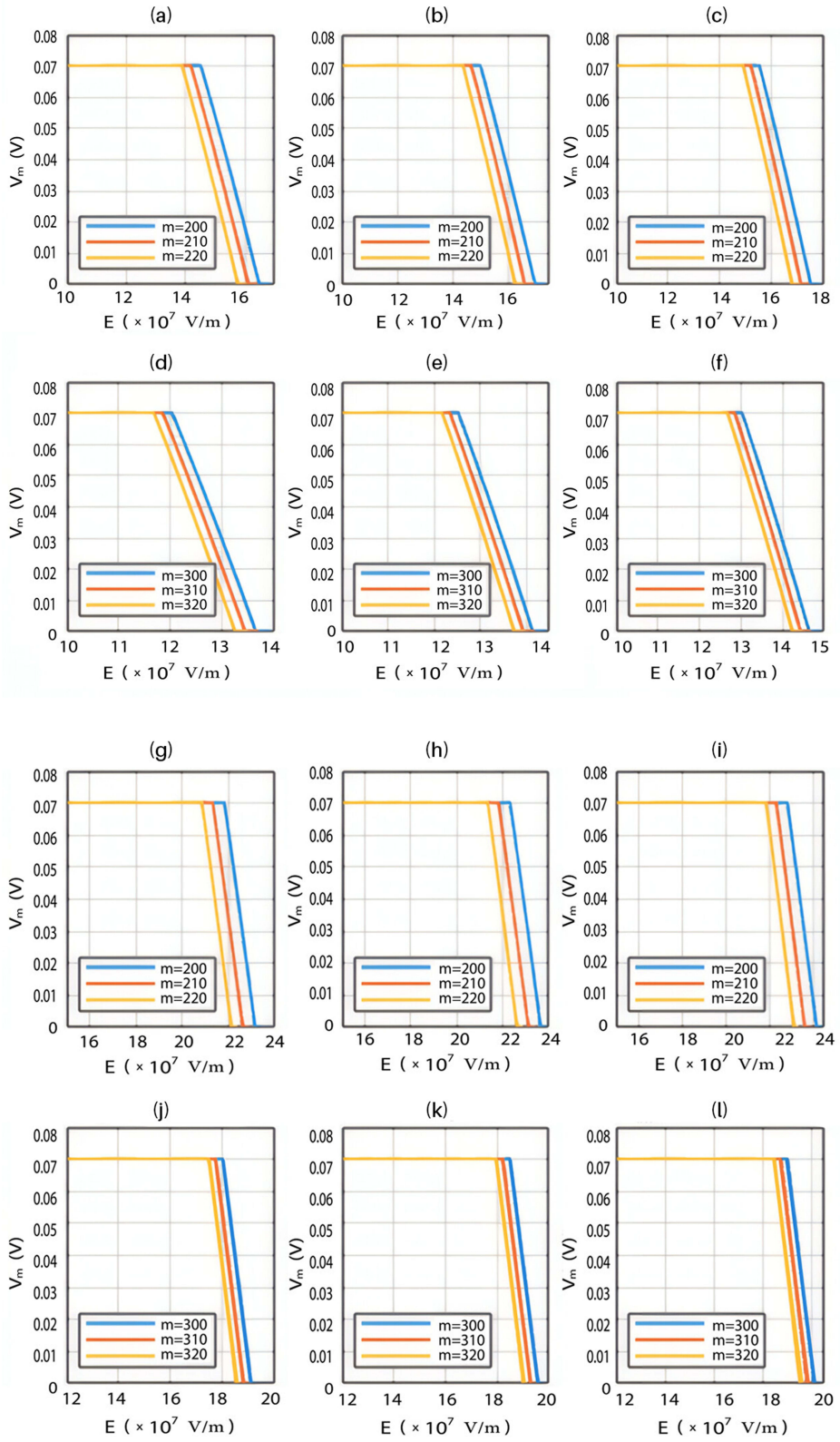

Figure 6 (**a–c**) **and** (**g–i**) The relationship between the strength of the external electric field E and the resting membrane potential under the influence of the quantum tunneling of both sodium and potassium ions at $E_{INT} = 1 \times 10^7$ V/m for (**a**) and (**g**), $E_{INT} = 1.5 \times 10^7$ V/m for (**b** and **h**) and $E_{INT} = 2 \times 10^7$ V/m for (**c** and **i**) and at three different values of m which are $m = 200$, $m = 210$ and $m = 220$. (**d–f**) and (**j–l**) The relationship between the strength of the electric field E and the resting membrane potential under the influence of the quantum tunneling of both sodium and potassium ions at $E_{INT} = 1 \times 10^7$ V/m for (**d** and **j**), $E_{INT} = 1.5 \times 10^7$ V/m for (**e** and **k**) and $E_{INT} = 2 \times 10^7$ V/m for (**f** and **l**) and at three different values of m which are $m = 300$, $m = 310$ and $m = 320$. The relationship is assessed at $G_{Na,K} = 5 \times 10^{-20}$ J for (**a–f**) and at $G_{Na,K} = 10 \times 10^{-20}$ J for (**g–l**) according to the quantum model without considering the influence of the external electric field on the kinetic energy of ions.

https://doi.org/10.2147/JPR.S566042

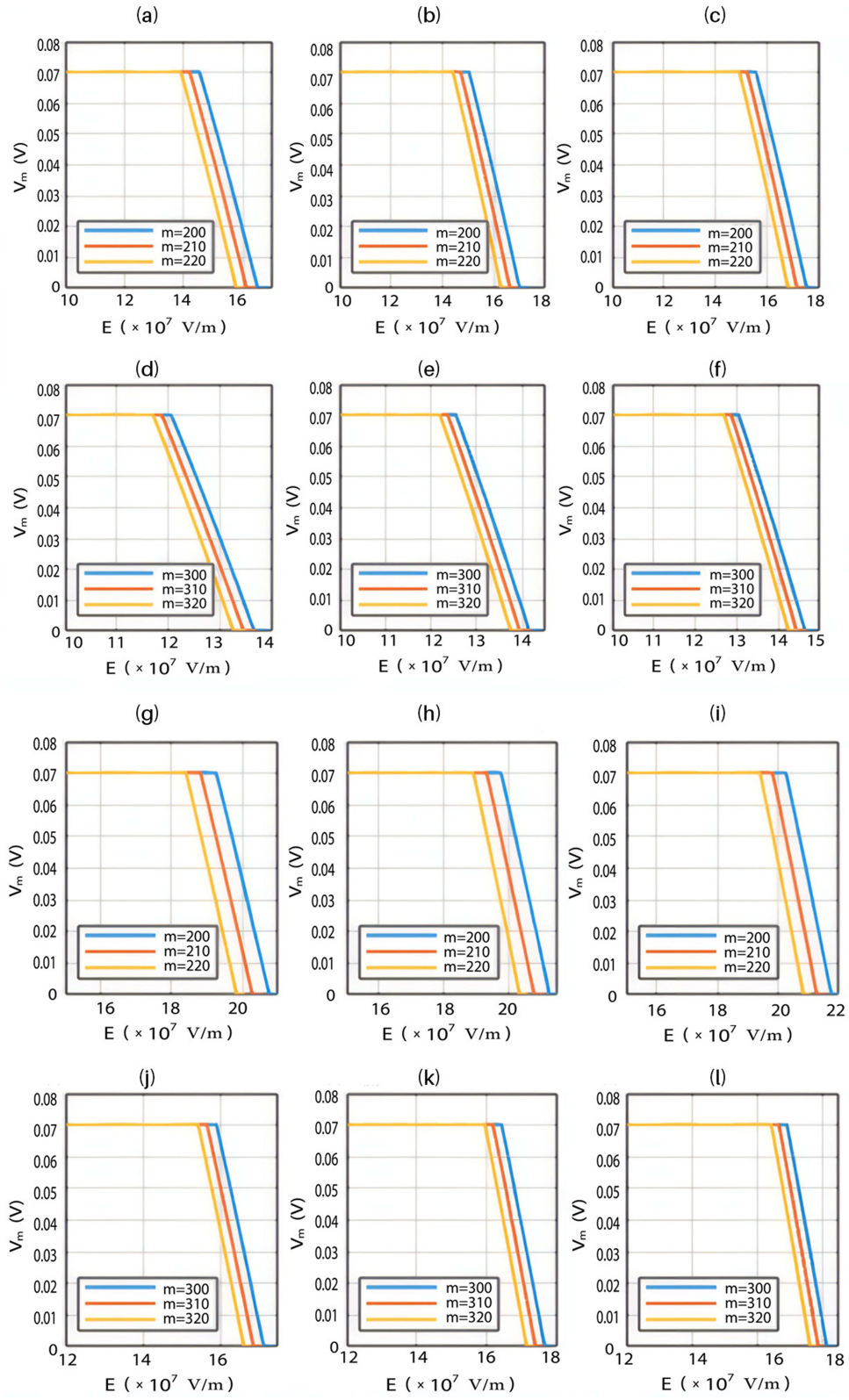

Figure 7 (**a–c**) and (**g–i**) The relationship between the strength of the external electric field E and the resting membrane potential under the influence of the quantum tunneling of both sodium and potassium ions at $E_{INT} = 1 \times 10^7$ V/m for (**a** and **g**), $E_{INT} = 1.5 \times 10^7$ V/m for (**b** and **h**) and $E_{INT} = 2 \times 10^7$ V/m for (**c** and **i**) and at three different values of m which are $m = 200$, $m = 210$ and $m = 220$. (**d–f**) and (**j–l**) The relationship between the strength of the external electric field E and the resting membrane potential under the influence of the quantum tunneling of both sodium and potassium ions at $E_{INT} = 1 \times 10^7$ V/m for (**d** and **j**), $E_{INT} = 1.5 \times 10^7$ V/m for (**e** and **k**) and $E_{INT} = 2 \times 10^7$ V/m for (**f** and **l**) and at three different values of m which are $m = 300$, $m = 310$ and $m = 320$. The relationship is investigated at $G_K = 5 \times 10^{-20}$ J and $G_{Na} = 10 \times 10^{-20}$ J for (**a–f**) and at $G_K = 8 \times 10^{-20}$ J and $G_{Na} = 10 \times 10^{-20}$ J for (**g–l**) according to the quantum model without considering the influence of the external electric field on the kinetic energy of ions.

For the purpose of comparison, the same investigation conducted in the previous section will be applied here, but in this case the influence of the external electric field on the kinetic energy of ions will be considered according to Equations (6)–(9) along with its influence on the barrier height of the hydrophobic gate. Accordingly, there are two cases:

1. If the direction of the external electric field is with the direction of the electric field of the neuronal membrane, the results will be as the following:

   The relationship between the external electric field and the membrane potential at $G_{Na.K} = 5 \times 10^{-20}$ J and $G_{Na.K} = 10 \times 10^{-20}$ J can be evaluated. See Figure 8.

The relationship between the electric field and the membrane potential at:
1. $G_K = 5 \times 10^{-20}$ J and $G_{Na} = 10 \times 10^{-20}$ J and,
2. $G_K = 8 \times 10^{-20}$ J and $G_{Na} = 10 \times 10^{-20}$ J can be evaluated. See Figure 9.

Each subplot in the figures above contains three graphs but they appear as one graph because they have very close values of membrane potential at each value of electric field.

1. If the direction of the external electric field is opposite to the direction of the internal electric field of the neuronal membrane, the results will be as the following:

   The relationship between the external electric field and the membrane potential at $G_{Na,K} = 5 \times 10^{-20}$ J and $G_{Na,K} = 10 \times 10^{-20}$ J can be evaluated. See Figure 10.

The relationship between the external electric field and the membrane potential at:
1. $G_K = 5 \times 10^{-20}$ J, and $G_{Na} = 10 \times 10^{-20}$ J, and
2. $G_K = 8 \times 10^{-20}$ J and $G_{Na} = 10 \times 10^{-20}$ J can be evaluated. See Figure 11.

The influence of the electric field induced by SCS on the neuron's membrane potential according to the classical transport.

Classical transport of ions through open channels is another mode of transport which occurs when the kinetic energy of ions is sufficient to overcome the barrier height of the closed gate. Based on the classical electrophysiology, the opening of sodium channels results in membrane depolarization, while the opening of potassium channels results in membrane hyperpolarization. In this section, we are going to study the influence of the external electric field on the classical transport of potassium and sodium ions and its effect on the neuron's membrane potential. This will aid in elaborating the differences between the quantum and classical transports and thus providing quantum mechanical aspects of the therapeutic effects of SCS to treat chronic neuropathic pain.

Based on Equation (13), the relationship between the strength of the external electric field and the membrane potential under the influence of opening the closed channels of both sodium and potassium ions can be investigated at $G_{Na,K} = 5 \times 10^{-20}$ J and $G_{Na,K} = 10 \times 10^{-20}$ J as in Figure 12.

Furthermore, the same relationship can be investigated when there is discrepancy between the values of the barrier height of potassium and sodium channels according to two possible cases:
1. $G_K = 5 \times 10^{-20}$ J and $G_{Na} = 10 \times 10^{-20}$ J and,
2. $G_K = 8 \times 10^{-20}$ J and $G_{Na} = 10 \times 10^{-20}$ J, which are assessed as in Figure 13.

To perform an objective comparison between the quantum and classical models in terms of energy efficiency, the following equation can be used:

$$r = \frac{\Delta Q}{\left(\frac{\Delta V}{\Delta E}\right)}, \tag{14}$$

 https://doi.org/10.2147/JPR.S566042

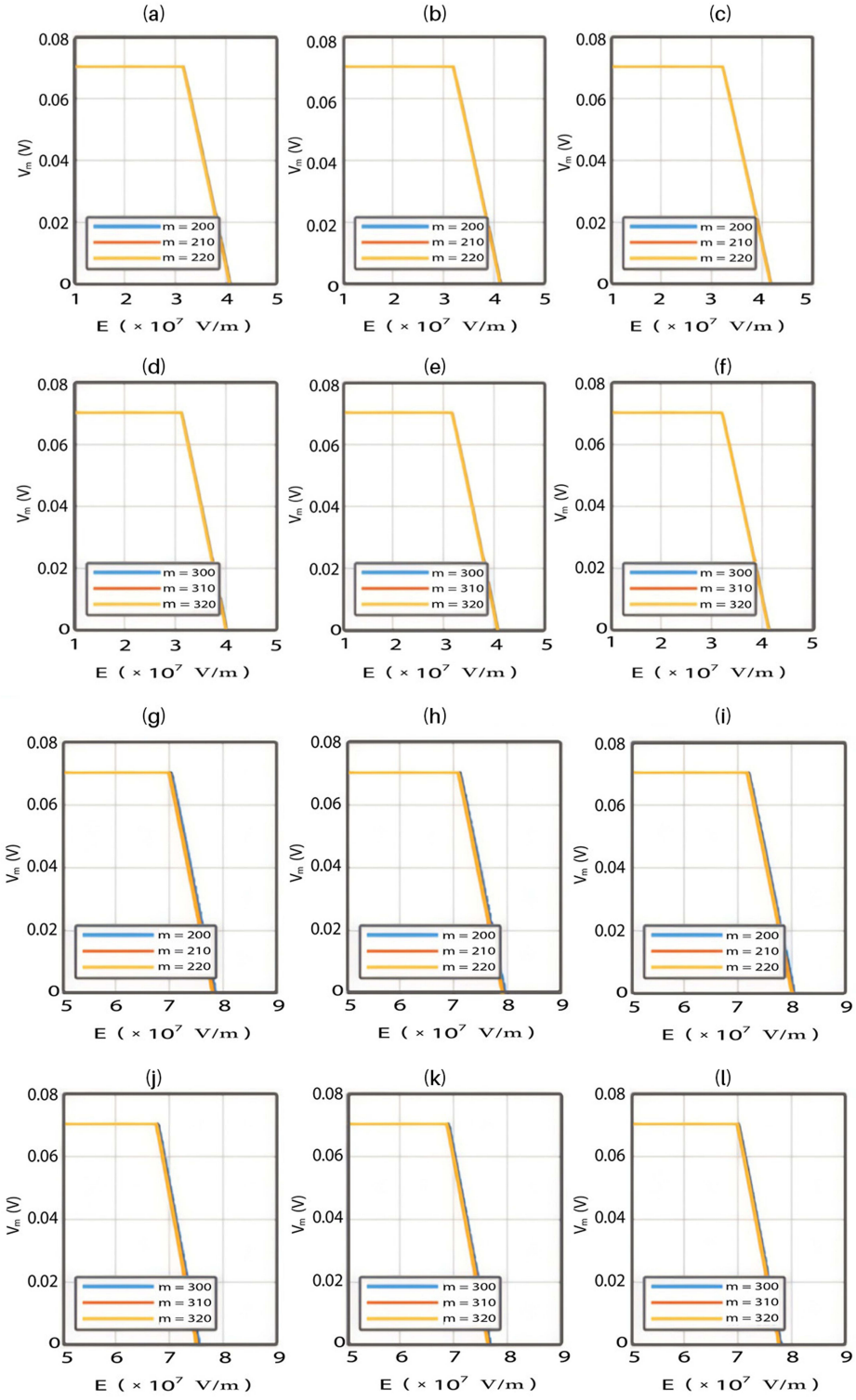

Figure 8 (**a–c**) and (**g–i**) The relationship between the strength of the external electric field and the resting membrane potential under the influence of the quantum tunneling of both sodium and potassium ions at $E_{INT} = 1 \times 10^7$ V/m for (**a** and **g**), $E_{INT} = 1.5 \times 10^7$ V/m for (**b** and **h**) and $E_{INT} = 2 \times 10^7$ V/m for (**c** and **i**) and at three different values of m which are $m = 200$, $m = 210$ and $m = 220$. (**d–f**) and (**j–l**) The relationship between the strength of the external electric field E and the resting membrane potential under the influence of the quantum tunneling of both sodium and potassium ions at $E_{INT} = 1 \times 10^7$ V/m for (**d** and **j**),$E_{INT} = 1.5 \times 10^7$ V/m for (**e** and **k**) and $E_{INT} = 2 \times 10^7$ V/m for (**f** and **l**) and at three different values of m which are $m = 300$, $m = 310$ and $m = 320$. The relationship is assessed at $G_{Na,K} = 5 \times 10^{-20}$ J for (**a–f**) and at $G_{Na,K} = 10 \times 10^{-20}$ J for (**g–l**) according to the quantum model and considering the influence of the external electric field on the kinetic energy of ions, which its direction is the same as the direction of the internal electric field of the neuronal membrane.

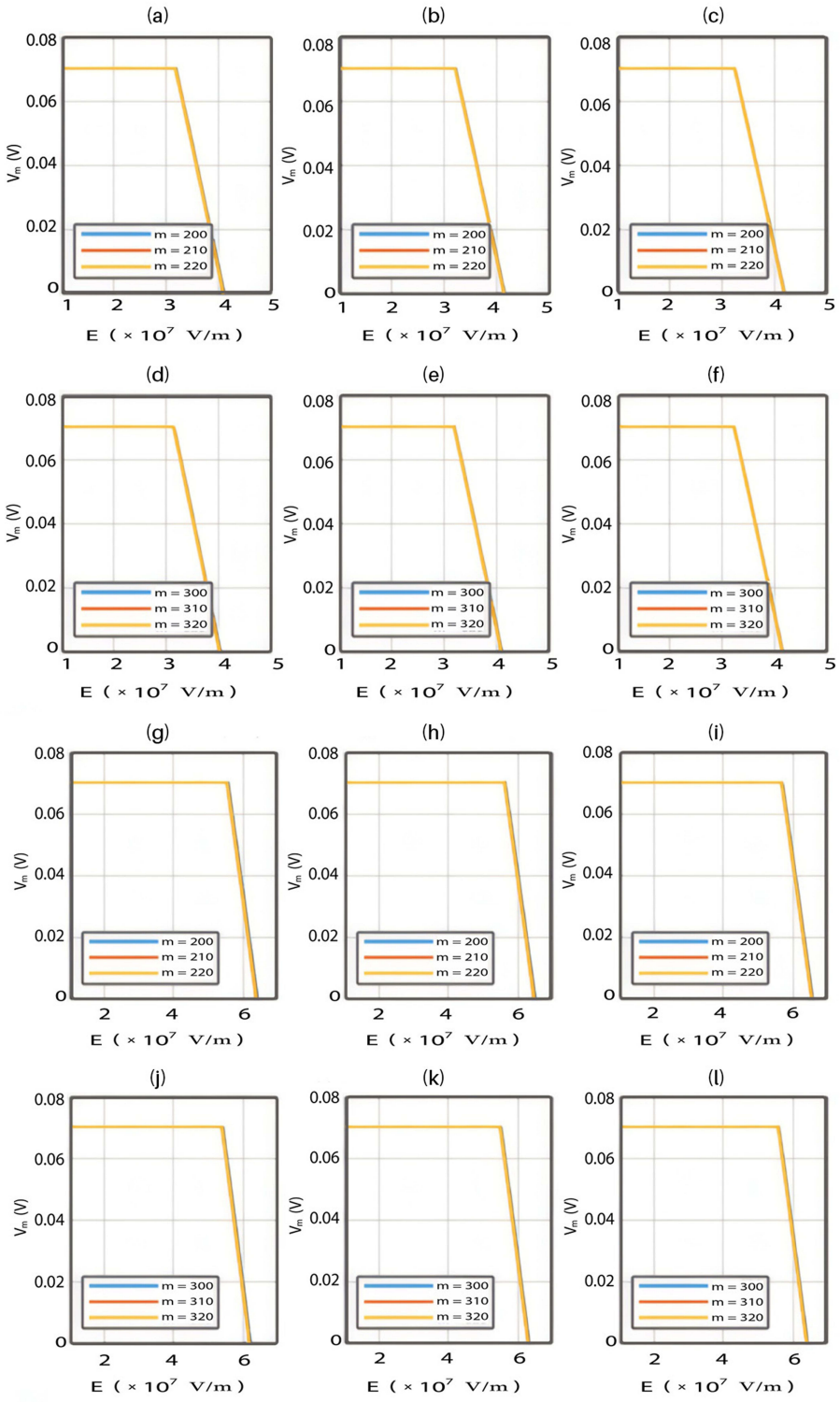

Figure 9 (**a**–**c**) and (**g**–**i**) The relationship between the strength of the external electric field E and the resting membrane potential under the influence of the quantum tunneling of both sodium and potassium ions at $E_{INT} = 1 \times 10^7$ V/m for (**a** and **g**), $E_{INT} = 1.5 \times 10^7$ V/m for (**b** and **h**) and $E_{INT} = 2 \times 10^7$ V/m for (**c** and **i**) and at three different values of m which are $m = 200$, $m = 210$ and $m = 220$. (**d**–**f**) and (**j**–**l**) The relationship between the strength of the external electric field E and the resting membrane potential under the influence of the quantum tunneling of both sodium and potassium ions at $E_{INT} = 1 \times 10^7$ V/m for (**d** and **j**),$E_{INT} = 1.5 \times 10^7$ mV/m for (**e** and **k**) and $E_{INT} = 2 \times 10^7$ V/m for (**f** and **l**) and at three different values of m which are $m = 300$, $m = 310$ and $m = 320$. The relationship is investigated at $G_K = 5 \times 10^{-20}$ J and $G_{Na} = 10 \times 10^{-20}$ J for (**a**–**f**) and at $G_K = 8 \times 10^{-20}$ J and $G_{Na} = 10 \times 10^{-20}$ J for (**g**–**l**) according to the quantum model and considering the influence of the external electric field on the kinetic energy of ions, which its direction is the same as the direction of the internal electric field of the neuronal membrane.

https://doi.org/10.2147/JPR.S566042

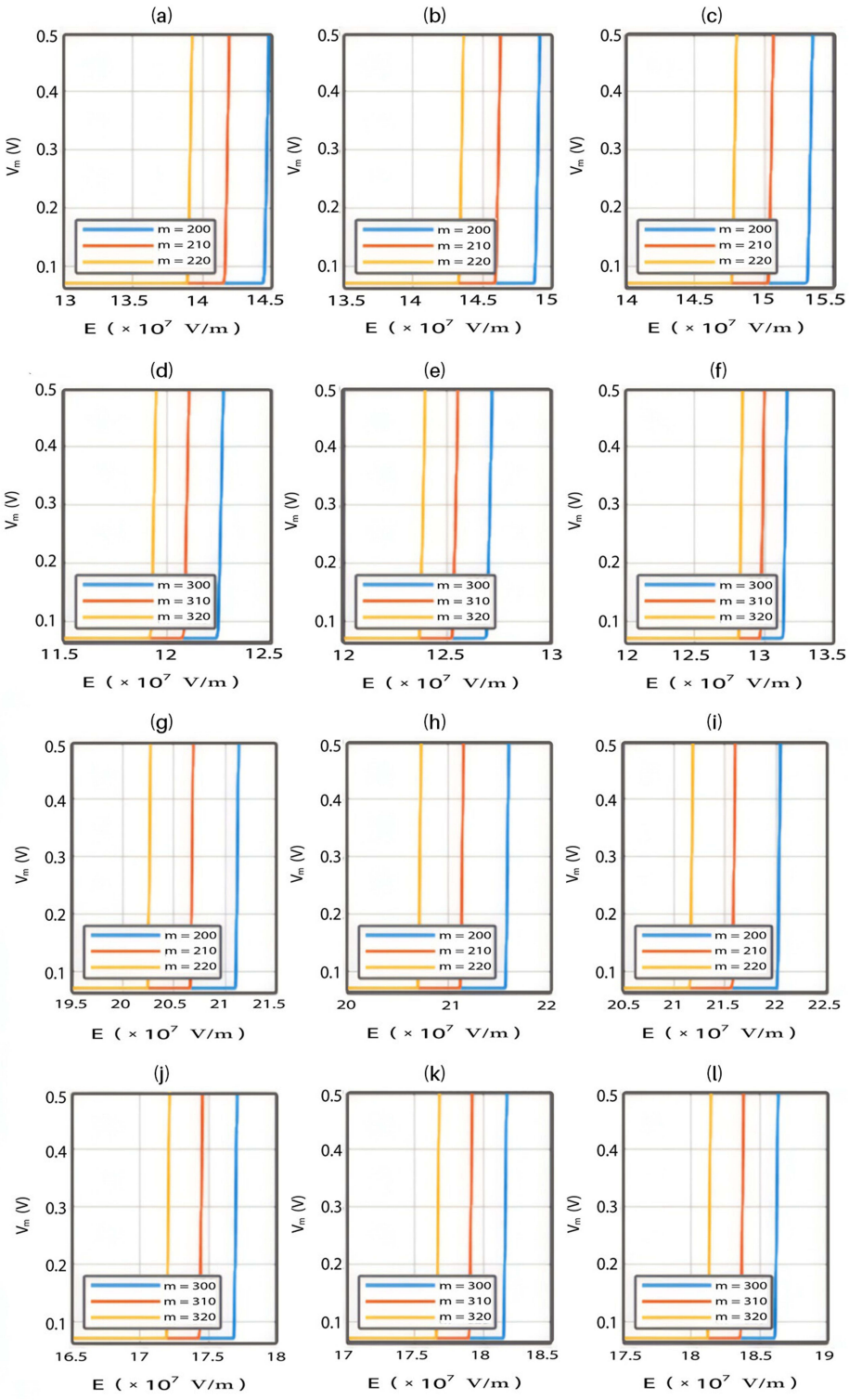

Figure 10 (**a–c**) and (**g–i**) The relationship between the strength of the external electric field E and the resting membrane potential under the influence of the quantum tunneling of both sodium and potassium ions at $E_{INT} = 1 \times 10^7$ V/m for (**a** and **g**), $E_{INT} = 1.5 \times 10^7$ V/m for (**b** and **h**) and $E_{INT} = 2 \times 10^7$ V/m **for** (**c** and **i**) and at three different values of m which are $m = 200$, $m = 210$ and $m = 220$. (**d–f**) and (**j–l**) The relationship between the strength of the external electric field E and the resting membrane potential under the influence of the quantum tunneling of both sodium and potassium ions at $E_{INT} = 1 \times 10^7$ V/m for (**d** and **j**), $E_{INT} = 1.5 \times 10^7$ V/m for (**e** and **k**) and $E_{INT} = 2 \times 10^7$ V/m for (**f** and **l**) and at three different values of m which are $m = 300$, $m = 310$ and $m = 320$. The relationship is assessed at $G_{Na,K} = 5 \times 10^{-20}$ J for (**a–f**) and at $G_{Na,K} = 10 \times 10^{-20}$ J for (**g–l**) according to the quantum model and considering the influence of the external electric field on the kinetic energy of ions, which its direction is the opposite of the direction of the internal electric field of the neuronal membrane.

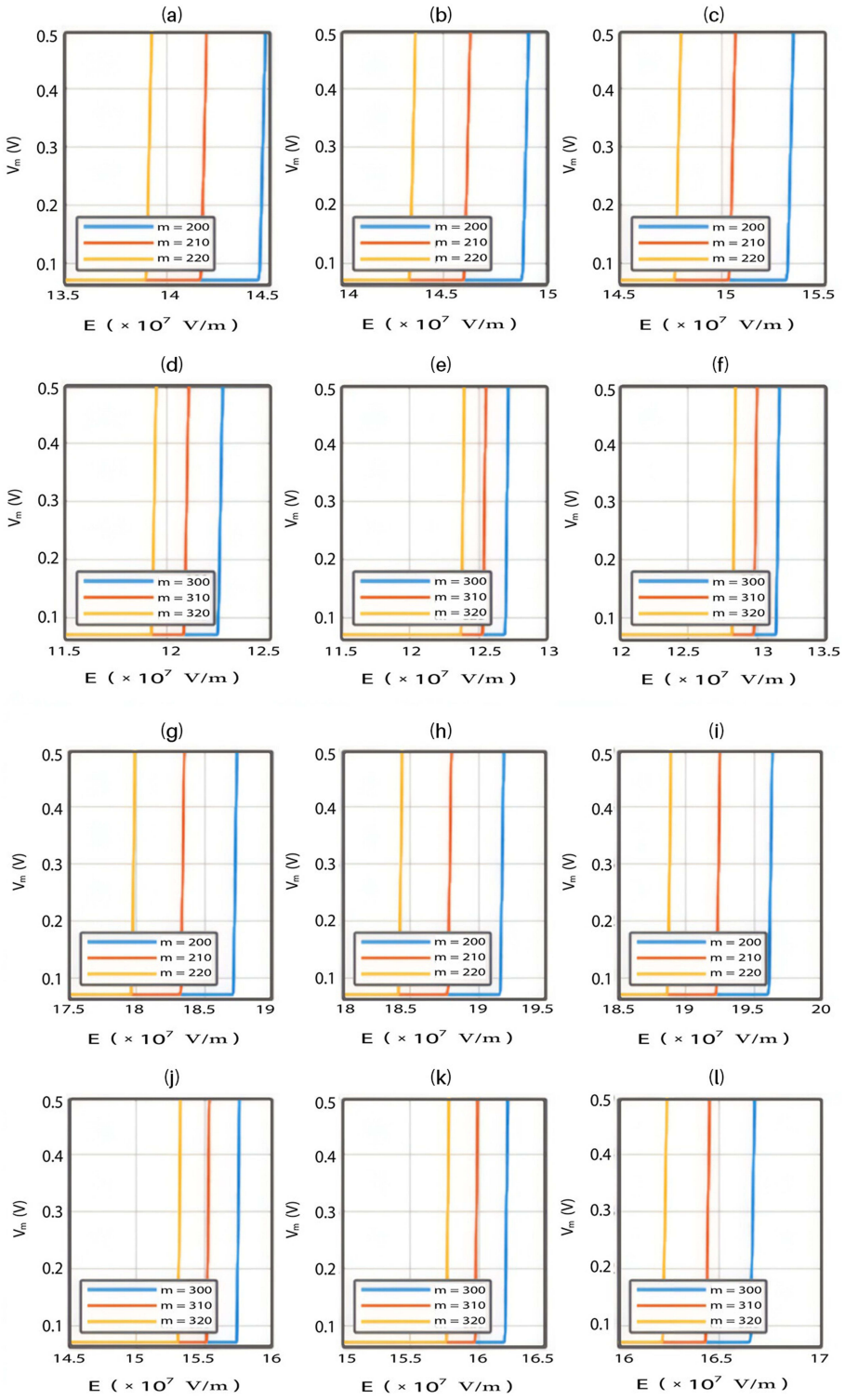

Figure 11 (**a–c**) and (**g–i**) The relationship between the strength of the external electric field E and the resting membrane potential under the influence of the quantum tunneling of both sodium and potassium ions at $E_{INT} = 1 \times 10^7$ V/m for (**a** and **g**), $E_{INT} = 1.5 \times 10^7$ V/m for (**b** and **h**) and $E_{INT} = 2 \times 10^7$ V/m for (**c** and **i**) and at three different values of m which are $m = 200$, $m = 210$ and $m = 220$. (**d–f**) and (**j–l**) The relationship between the strength of the external electric field E and the resting membrane potential under the influence of the quantum tunneling of both sodium and potassium ions at $E_{INT} = 1 \times 10^7$ V/m for (**d** and **j**), $E_{INT} = 1.5 \times 10^7$ V/m for (**e** and **k**) and $E_{INT} = 2 \times 10^7$ V/m for (**f** and **l**) and at three different values of m which are $m = 300$, $m = 310$ and $m = 320$. The relationship is investigated at $G_K = 5 \times 10^{-20}$ J and $G_{Na} = 10 \times 10^{-20}$ J for (**a–f**) and at $G_K = 8 \times 10^{-20}$ J and $G_{Na} = 10 \times 10^{-20}$ J for (**g–l**) according to the quantum model and considering the influence of the external electric field on the kinetic energy of ions, which its direction is the opposite of the direction of the internal electric field of the neuronal membrane.

https://doi.org/10.2147/JPR.S566042

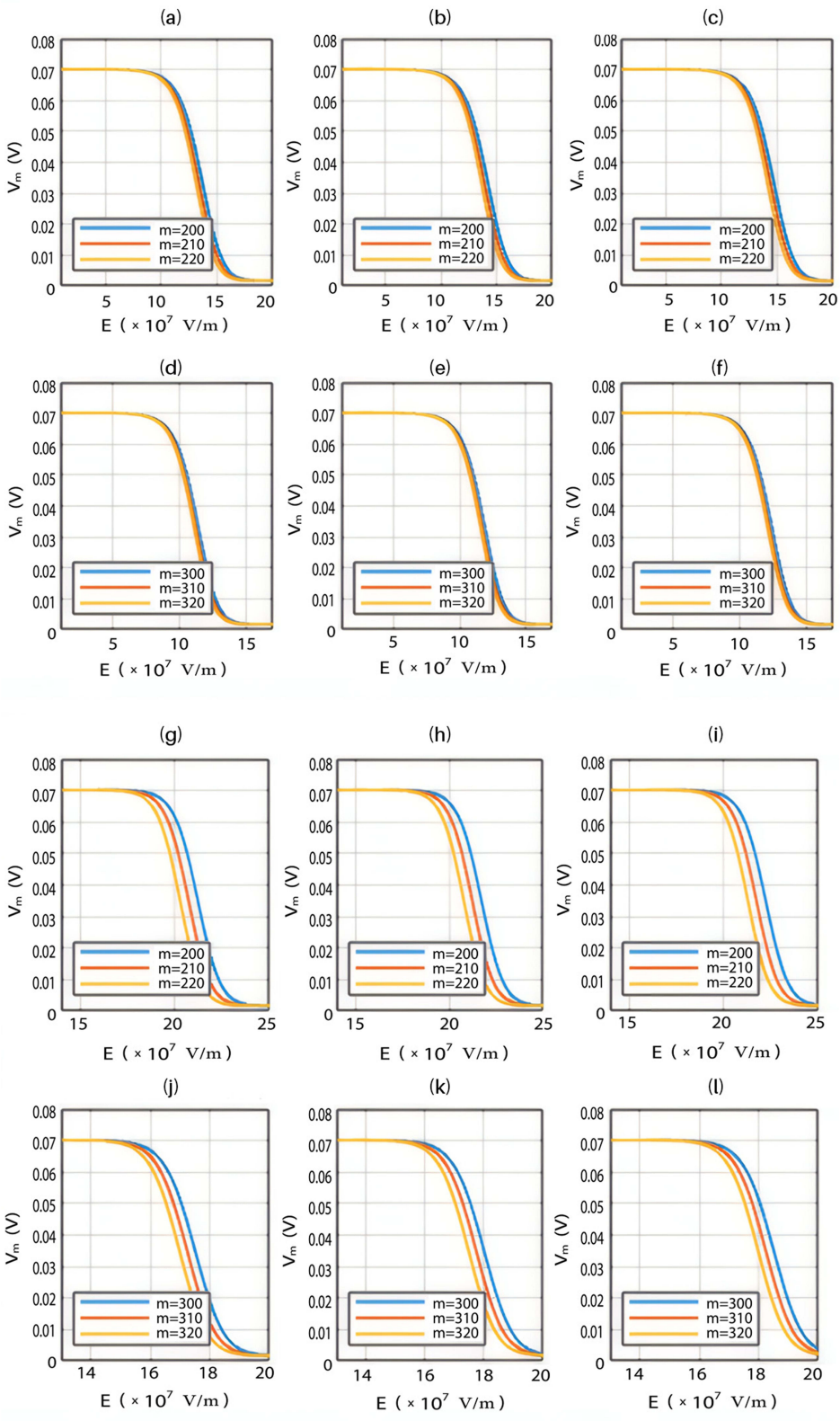

Figure 12 (**a–c**) and (**g–i**) The relationship between the strength of the external electric field E and the resting membrane potential under the influence of the opening of both sodium and potassium channels at $E_{INT} = 1 \times 10^7$ V/m for (**a** and **g**) $E_{INT} = 1.5 \times 10^7$ V/m for (**b** and **h**) and $E_{INT} = 2 \times 10^7$ V/m for (**c** and **i**) and at three different values of m which are $m = 200$, $m = 210$ and $m = 220$. (**d–f**) and (**j–l**) The relationship between the strength of the external electric field E and the resting membrane potential under the influence of the opening of both sodium and potassium channels at $E_{INT} = 1 \times 10^7$ V/m for (**d** and **j**), $E_{INT} = 1.5 \times 10^7$ V/m for (**e** and **k**) and $E_{INT} = 2 \times 10^7$ V/m for (**f** and **l**) and at three different values of m which are $m = 300$, $m = 310$ and $m = 320$. The relationship is assessed at $G_{Na,K} = 5 \times 10^{-20}$ J for (**a–f**) and at $G_{Na,K} = 10 \times 10^{-20}$ J for (**g–l**) according to the classical model.

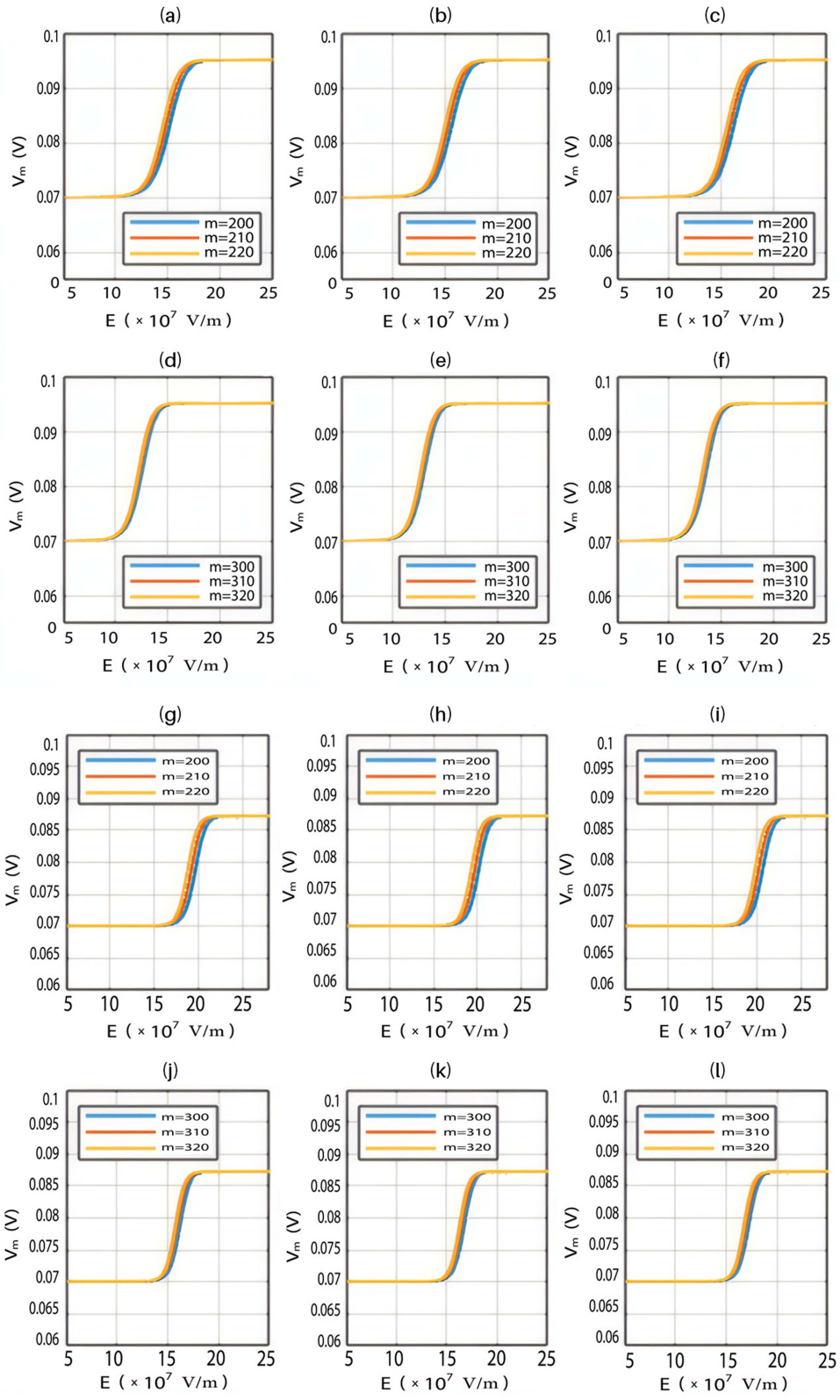

Figure 13 (**a–c**) and (**g–i**) The relationship between the strength of the external electric field E and the resting membrane potential under the influence of the opening of both sodium and potassium channels at $E_{INT} = 1 \times 10^7$ V/m for (**a** and **g**), $E_{INT} = 1.5 \times 10^7$ V/m for (**b** and **h**) and $E_{INT} = 2 \times 10^7$ V/m for (**c** and **i**) and at three different values of m which are $m = 200$, $m = 210$ and $m = 220$. (**d–f**) and (**j–i**) The relationship between the strength of the external electric field E and the resting membrane potential under the influence of the opening of both sodium and potassium channels at $E_{INT} = 1 \times 10^7$ V/m for (**d** and **j**), $E_{INT} = 1.5 \times 10^7$ V/m for (**e** and **k**) and $E_{INT} = 2 \times 10^7$ V/m for (**f** and **i**) and at three different values of m which are $m = 300$, $m = 310$ and $m = 320$. The relationship is assessed at $G_K = 5 \times 10^{-20}$ J and $G_{Na} = 10 \times 10^{-20}$ J for (**a–f**) and at $G_K = 8 \times 10^{-20}$ J and $G_{Na} = 10 \times 10^{-20}$ J for (**g–l**) according to the classical model.

https://doi.org/10.2147/JPR.S566042

where r is the average energy (in Joule) needed to change the membrane potential 0.01 V per 1×10^7 V/m intensity of external electric field, ΔQ is the difference in the energy demand between the initial and final states, ΔV is the difference in the membrane potential between the initial and final states, and ΔE is the difference in the intensity of the external electric field between the initial and final states.

For the quantum model and according to Figures 6–9, the initial state is the beginning of the graph to drop from 0.07 V until 0 V, which represents the final state. According to Equation (2), the energy needed ΔQ to induce depolarization is the kinetic energy of the ion $KE = qV_m + \frac{1}{2}K_BT$.

For the classical model and according to Figure 12, the shape of the graph by which the membrane potential changes with the electric field is different from the quantum model. The shape of the line in the classical model is a sigmoid shape while it is inverse linear relationship in the quantum model. Therefore, the initial and the final states in the sigmoid shape are less demarcated since there are two plateaus in which the membrane potential changes by very small values with respect to the electric field. Hence, we choose the initial and final states so that they include the majority of the change in the potential without including a major proportion of the two plateaus. The initial state will be 0.069 V and the final state will be 0.005 V. Moreover, the energy needed to induce depolarization is G^*, which is the barrier height of the closed gate under the influence of the external electric field.

Tables 2–5 contain the r values for the quantum model without considering the influence of the external electric field on the kinetic energy and Tables 6–9 contain the r values for the quantum model considering the influence of the external electric field on the kinetic energy of ions, while Tables 10 and 11 contain r values for the classical model.

Figures 10, 11 and 13 were not included in the tables above because their outcome was hyperpolarization instead of depolarization because our major interest in the present study is depolarization as it reflects the stimulation effect of SCS. Comparing these tables together, the r values of the quantum model are 4 to 30 times lower than the r values of the classical model. This is due to two reasons: 1) for the same set of m and E_{INT} values, G^* values are always higher than the kinetic energy of the ion KE and 2) for the same set of m and E_{INT} values; the range of electric field required for depolarization is narrower in the quantum model compared to the classical model.

In the previous plots, we performed sensitivity testing focusing on how the membrane potential changes by varying the range of the external electric field at different conditions and at specified values of other parameters. However, we are going to perform several sensitivity analyses to investigate how the membrane potential changes by varying the range of one parameter while holding other parameters at their average value. We determined the ranges of each parameter based on the minimum and maximum values used in the model and the average value is calculated as the average value of the minimum and maximum values. Additionally, we are going to conduct the sensitivity analysis for the four cases we discussed before, which are: 1) The quantum model in which the effect of the external electric field on the kinetic energy

Table 2 It Contains the r Values When $G_{Na,K} = 5 \times 10^{-20}$ J at Different Values of m and E_{INT} According to Figure 6. The r Values in the Table are in the Unit of 10^{-20} J/0.01V/10^7 V.m^{-1}

m Value	E_{INT}		
	1	1.5	2
200	0.34	0.30	0.32
210	0.29	0.32	0.32
220	0.37	0.32	0.30
300	0.26	0.26	0.26
310	0.27	0.26	0.26
320	0.26	0.24	0.26

Table 3 It Contains the r Values when $G_{Na,K} = 10 \times 10^{-20}$ J at Different Values of m and E_{INT} According to Figure 6. The r Values in the Table are in the Unit of 10^{-20} J/0.01V/10^{7} V.m^{-1}

m Value	E_{INT}		
	1	1.5	2
200	0.22	0.21	0.22
210	0.22	0.22	0.22
220	0.22	0.22	0.21
300	0.19	0.19	0.19
310	0.18	0.19	0.18
320	0.19	0.18	0.18

Table 4 It Contains the r Values When $G_K = 5 \times 10^{-20}$ J and $G_{Na} = 10 \times 10^{-20}$ J at Different Values of m and E_{INT} According to Figure 7. The r Values in the Table are in the Unit of 10^{-20} J/0.01V/10^{7} V.m^{-1}

m Value	E_{INT}		
	1	1.5	2
200	0.32	0.32	0.32
210	0.34	0.32	0.32
220	0.32	0.32	0.32
300	0.26	0.26	0.26
310	0.26	0.26	0.26
320	0.24	0.26	0.26

Table 5 It Contains the r Values When $G_K = 8 \times 10^{-20}$ J and $G_{Na} = 10 \times 10^{-20}$ J at Different Values of m and E_{INT} according to Figure 7. The r Values in the Table are in the Unit of 10^{-20} J/0.01V/10^{7} V.m^{-1}

m Value	E_{INT}		
	1	1.5	2
200	0.24	0.24	0.24
210	0.26	0.26	0.24
220	0.22	0.22	0.24
300	0.19	0.19	0.19
310	0.19	0.21	0.19
320	0.19	0.19	0.19

https://doi.org/10.2147/JPR.S566042

Table 6 It Contains the r Values When $G_{Na,K} = 5 \times 10^{-20}$ J at Different Values of m and E_{INT} According to Figure 8. The r Values in the Table are in the Unit of 10^{-20} J/0.01V/10^7 V.m^{-1}

m Value	E_{INT}		
	1	1.5	2
200	0.16	0.16	0.16
210	0.16	0.16	0.16
220	0.16	0.16	0.16
300	0.15	0.16	0.16
310	0.15	0.16	0.16
320	0.15	0.16	0.16

Table 7 It Contains the r Values when $G_{Na,K} = 10 \times 10^{-20}$ J at Different Values of m and E_{INT} According to Figure 8. The r Values in the Table are in the Unit of 10^{-20} J/0.01V/10^7 V.m^{-1}

m Value	E_{INT}		
	1	1.5	2
200	0.15	0.15	0.15
210	0.15	0.15	0.15
220	0.15	0.15	0.15
300	0.14	0.13	0.14
310	0.14	0.13	0.14
320	0.14	0.13	0.14

Table 8 It Contains the r Values When $G_K = 5 \times 10^{-20}$ J and $G_{Na} = 10 \times 10^{-20}$ J at Different Values of m and E_{INT} according to Figure 9. The r Values in the Table are in the Unit of 10^{-20} J/0.01V/10^7 V.m^{-1}

m Value	E_{INT}		
	1	1.5	2
200	0.15	0.16	0.17
210	0.15	0.16	0.17
220	0.15	0.16	0.17
300	0.16	0.15	0.16
310	0.16	0.15	0.16
320	0.16	0.15	0.16

Table 9 It Contains r Values When $G_K = 8 \times 10^{-20}$ J and $G_{Na} = 10 \times 10^{-20}$ J at Different Values of m and E_{INT} according to Figure 9. The r Values in the Table are in the Unit of 10^{-20} J/0.01V/10^7 V.m^{-1}

m Value	E_{INT}		
	1	1.5	2
200	0.15	0.15	0.16
210	0.15	0.15	0.16
220	0.15	0.15	0.16
300	0.16	0.14	0.15
310	0.16	0.14	0.15
320	0.16	0.14	0.15

Table 10 It Contains the r Values When $G_{Na,K} = 5 \times 10^{-20}$ J at Different Values of m and E_{INT} According to Figure 12. The r Values in the Table are in the Unit of 10^{-20} J/0.01V/10^7 V.m^{-1}

m Value	E_{INT}		
	1	1.5	2
200	3.89	4.21	3.13
210	3.74	3.74	3.86
220	3.63	3.62	3.63
300	3.35	3.02	3.35
310	3.01	3.04	3.34
320	3.05	3.01	3.05

Table 11 It Contains the r Values When $G_{Na,K} = 10 \times 10^{-20}$ J at Different Values of m and E_{INT} According to Figure 12. The r Values in the Table are in the Unit of 10^{-20} J/0.01V/10^7 V.m^{-1}

m Value	E_{INT}		
	1	1.5	2
200	2.20	2.25	2.19
210	2.06	2.06	2.26
220	2.06	2.06	2.06
300	1.98	1.72	1.88
310	1.75	1.75	1.75
320	1.77	1.73	1.73

https://doi.org/10.2147/JPR.S566042

Table 12 The Changes in the Membrane Potential According to the Range of One Parameter While Holding Other Parameters Constant at Their Average Values and for the First Case

Parameter	Range	Average Value	V_m Range
External electric field E	$(11.5-24)\times10^{7}$ V/m	17.75×10^{7} V/m	0.07 V to -7.96×10^{-5} V, see Figure 14a
Intrinsic electric field E_{INT}	$(1-2)\times10^{7}$ V/m	1.5×10^{7} V/m	0.05 V to -9.68×10^{-5} V, see Figure 14b
Barrier height for potassium channels G_K	$(5-10)\times10^{-20}$ J	7.5×10^{-20} J	0.025 V to 8.87×10^{-5} V, see Figure 14c
Barrier height for sodium channels G_{Na}	$(5-10)\times10^{-20}$ J	7.5×10^{-20} J	0.026 V to −0.013 V, see Figure 14d
Coupling factor m	$(200-320)\times10^{-20}$ J.nm^2.V^{-2}	260×10^{-20} J.nm^2.V^{-2}	0.07 V to -8×10^{-5} V, see Figure 14e

of ions is not considered. 2) The quantum model in which the effect of the external electric field on the kinetic energy of ions is considered and its direction is the same as the direction of the internal electric field of the neuronal membrane. 3) The quantum model in which the effect of the external electric field on the kinetic energy of ions is considered and its direction is opposite to the direction of the internal electric field of the neuronal membrane. 4) The classical model.

The sensitivity analysis focusing on the changes in the membrane potential with respect to all parameters is investigated for the first case. See Table 12 and Figure 14.

The sensitivity analysis focusing on the changes in the membrane potential with respect to all parameters is investigated for the second case. See Table 13 and Figure 15.

The sensitivity analysis focusing on the changes in the membrane potential with respect to all parameters is investigated for the third case. See Table 14 and Figure 16.

The sensitivity analysis focusing on the changes in the membrane potential with respect to all parameters is investigated for the fourth case. See Table 15 and Figure 17.

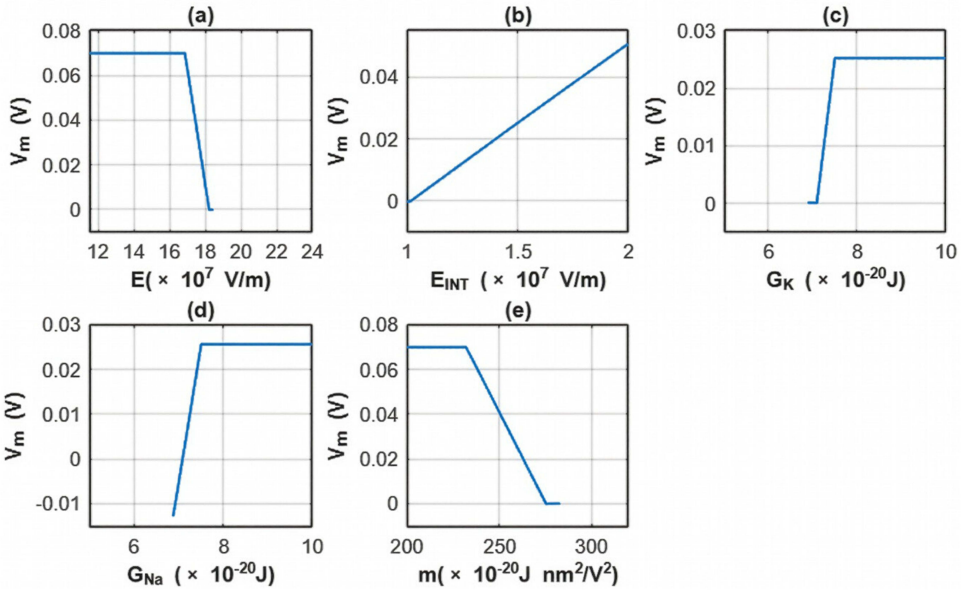

Figure 14 The changes in the membrane potential across the range of one parameter while holding other parameters constant at their average value for the first case. (**a**) The sensitivity analysis is done according to the range of the external electric field while holding other parameters constant at their average values. (**b**) The sensitivity analysis is done according to the range of the intrinsic electric field while holding other parameters constant at their average values. (**c**) The sensitivity analysis is done according to the range of the barrier height of potassium channel while holding other parameters constant at their average values. (**d**) The sensitivity analysis is done according to the range of the barrier height of sodium channel while holding other parameters constant at their average values. (**e**) The sensitivity analysis is done according to the range of the m value while holding other parameters constant at their average values.

 https://doi.org/10.2147/JPR.S566042

Table 13 The Changes in the Membrane Potential According to the Range of One Parameter While Holding Other Parameters Constant at Their Average Values and for the second Case

Parameter	Range	Average Value	V_m Range
External electric field E	$(3-8)\times 10^{7}$ V/m	5.5×10^{7} V/m	0.07 V to – 0.18 V, see Figure 15a
Intrinsic electric field E_{INT}	$(1-2)\times 10^{7}$ V/m	1.5×10^{7} V/m	0.046 V to 0.033 V, see Figure 15b
Barrier height for potassium channels G_K	$(5-10)\times 10^{-20}$ J	7.5×10^{-20} J	0.04 V to - 0.11 V, see Figure 15c
Barrier height for sodium channels G_{Na}	$(5-10)\times 10^{-20}$ J	7.5×10^{-20} J	0.042 V to −0.11V, See Figure 15d
Coupling factor m	$(200-320)\times 10^{-20}$ J.nm^2.V^{-2}	260×10^{-20} J.nm^2.V^{-2}	0.046 V to 0.034 V, see Figure 15e

Discussion

SCS delivers electric charges to the regions in the spinal cord, and they generate electric fields that can influence the neuronal excitability. One of the most important molecular targets that are affected by electric fields is ion channels which are central in determining the excitability of neurons by controlling the electric membrane potential of neurons. K2P and NALCN channels are two crucial types of ion channels which are key players in determining the resting membrane potential by setting the leaky or background conductance of potassium and sodium ions, respectively. Therefore, exploring the impact of electric fields on these channels and their therapeutic effect to treat chronic neuropathic pain is promising in order to understand the mechanism of action of SCS. There are two major approaches to investigate the influence of electric fields on these channels, which are the classical and quantum approaches. In the present study, we used the mathematical model of ions quantum tunneling through closed gates to search for possible mechanisms of SCS. In addition, the classical transport of ions through open channels is investigated to delineate the differences between the quantum and classical approaches.

According to the present model, when the electric field decreases the energy barrier of the hydrophobic gate, the probability of quantum tunneling increases. As a result, the quantum unitary conductance and quantum membrane

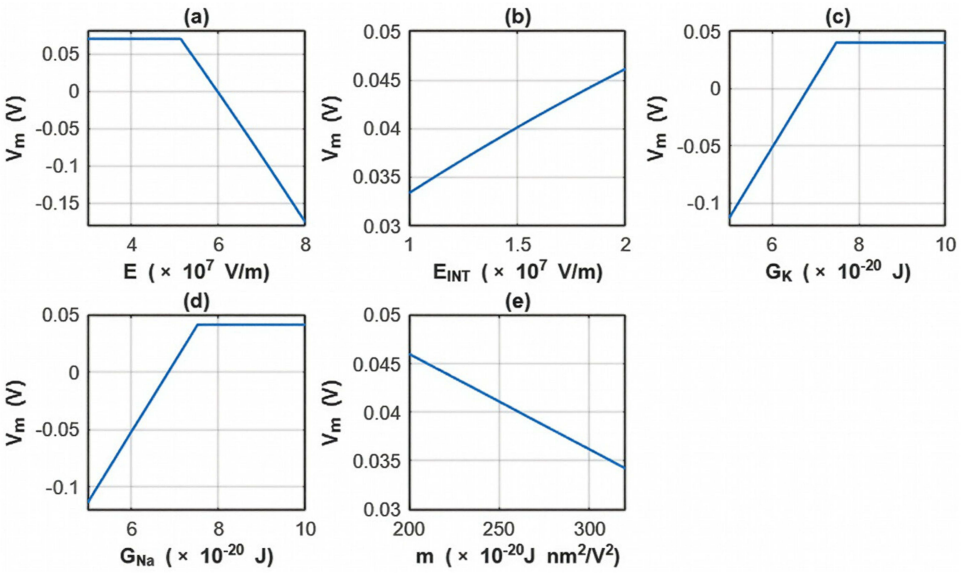

Figure 15 The changes in the membrane potential across the range of one parameter while holding other parameters constant at their average value for the second case. (**a**) The sensitivity analysis is done according to the range of the external electric field while holding other parameters constant at their average values. (**b**) The sensitivity analysis is done according to the range of the intrinsic electric field while holding other parameters constant at their average values. (**c**) The sensitivity analysis is done according to the range of the barrier height of potassium channel while holding other parameters constant at their average values. (**d**) The sensitivity analysis is done according to the range of the barrier height of sodium channel while holding other parameters constant at their average values. (**e**) The sensitivity analysis is done according to the range of the m value while holding other parameters constant at their average values.

https://doi.org/10.2147/JPR.S566042

Table 14 The Changes in the Membrane Potential According to the Range of One Parameter While Holding Other Parameters Constant at Their Average Values and for the Third Case

Parameter	Range	Average Value	V_m Range
External electric field E	$(11.5-22)\times10^{7}$ V/m	16.75×10^{7} V/m	0.07 V to 1.3 V, see Figure 16a
Intrinsic electric field E_{INT}	$(1-2)\times10^{7}$ V/m	1.5×10^{7} V/m	0.07 V to 1.25 V, see Figure 16b
Barrier height for potassium channels G_K	$(5-10)\times10^{-20}$ J	7.5×10^{-20} J	1.251 V to 1.256 V, see Figure 16c
Barrier height for sodium channels G_{Na}	$(5-10)\times10^{-20}$ J	7.5×10^{-20} J	1.251 V to 1.256 V, see Figure 16d
Coupling factor m	$(200-320)\times10^{-20}$ J.nm^2.V^{-2}	260×10^{-20} J.nm^2.V^{-2}	0.07 V to 1.25 V, see Figure 16e

conductance of sodium and potassium ions will also increase. There are several factors that determine the relationship between the electric field induced by SCS and the probability of quantum tunneling and the quantum conductance. These factors include the strength of the external electric field E,E_{INT}, and the m value. As the strength of the external electric field E and the m value increase, the hydration probability of the pore increases and the potential energy barrier of the hydrophobic gate decreases. On the other hand, as E_{INT} increases, the hydration probability decreases, and the drop in the potential energy barrier will be attenuated. Furthermore, the tunneling probability and the quantum conductance of extracellular cations, including potassium and sodium ions, are much higher than these of intracellular cations. This is attributed to the higher kinetic energy of extracellular cations while passing across the membrane potential of neurons, which is negative inside with regard to outside, until reaching the intracellular hydrophobic gate. Consequently, in the case that the influence of the external electric field on the kinetic energy of ions is not considered it is expected that an inward cationic flow of both potassium and sodium ions is generated and this influx can depolarize the membrane potential of neurons. According to Figures 6 and 7, the quantum tunneling of both sodium and potassium ions can depolarize the resting membrane potential under the influence of electric fields generated by the SCS. The strength of the

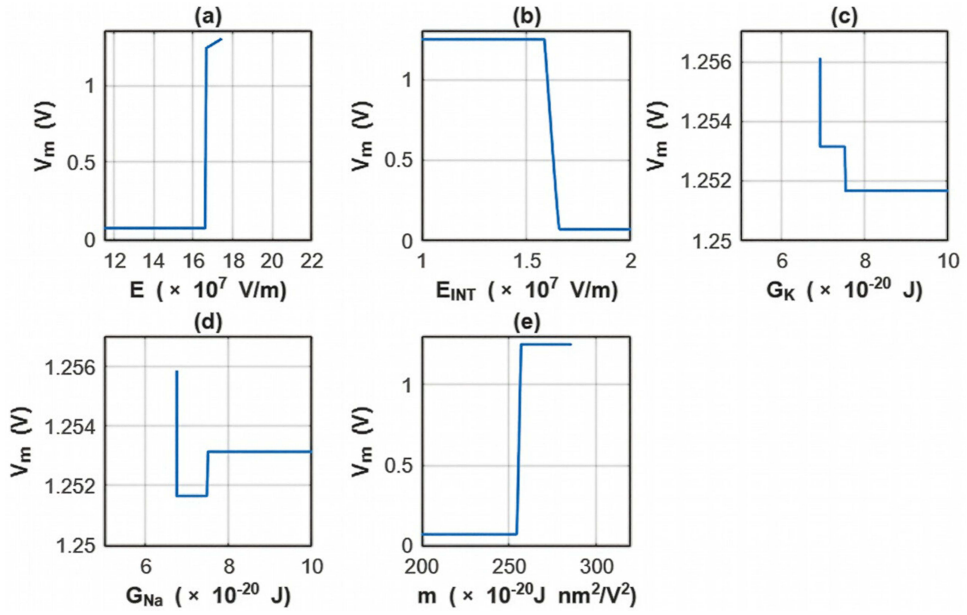

Figure 16 The changes in the membrane potential across the range of one parameter while holding other parameters constant at their average value for the third case. (**a**) The sensitivity analysis is done according to the range of the external electric field while holding other parameters constant at their average values. (**b**) The sensitivity analysis is done according to the range of the intrinsic electric field while holding other parameters constant at their average values. (**c**) The sensitivity analysis is done according to the range of the barrier height of potassium channel while holding other parameters constant at their average values. (**d**) The sensitivity analysis is done according to the range of the barrier height of sodium channel while holding other parameters constant at their average values. (**e**) The sensitivity analysis is done according to the range of the m value while holding other parameters constant at their average values.

Table 15 The Changes in the Membrane Potential According to the Range of One Parameter While Holding Other Parameters Constant at Their Average Values and for the Fourth Case

Parameter	Range	Average Value	V_m Range
External electric field E	$(8-25)\times10^{7}$ V/m	16.5×10^{7} V/m	0.07 V to 0.001 V, see Figure 17a
Intrinsic electric field E_{INT}	$(1-2)\times10^{7}$ V/m	1.5×10^{7} V/m	0.041 V to 0.016 V, see Figure 17b
Barrier height for potassium channels G_K	$(5-10)\times10^{-20}$ J	7.5×10^{-20} J	0.092 V to 0.019 V, see Figure 17c
Barrier height for sodium channels G_{Na}	$(5-10)\times10^{-20}$ J	7.5×10^{-20} J	0.075 V to −0.059 V, see Figure 17d
Coupling factor m	$(200-320)\times10^{-20}$ J.nm^2.V^{-2}	260×10^{-20} J.nm^2.V^{-2}	0.064 V to 0.0036 V, see Figure 17e

electric field required to depolarize the membrane potential varies based on several factors as we mentioned before. As the barrier height of the closed gate increases, the required strength of the electric field increases. In addition, as the *m* value increases, the required strength of the electric field decreases, while as E_{INT} value increases, the required strength of the electric field increases. Generally, the range of the external electric field generated by SCS should be within $(11.5-24)\times10^{7}$ V/m to depolarize the membrane potential via quantum tunneling of ions. The ability of potassium ions to depolarize the membrane potential may be unique to the quantum approach if it is compared with the classical approach which predicts the occurrence of hyperpolarization instead of depolarization. However, when the influence of the external electric field on the kinetic energy of ions is considered, there are two effects on the membrane potential that can be observed according to Figures 8–11. The first effect is depolarization and the second effect is hyperpolarization. The depolarization is expected to occur when the direction of the external electric field is the same as the direction of the internal electric field of the neuronal membrane according to Figures 8 and 9. In this case, the depolarization occurs at lower values of electric field intensity compared with the case in which only the influence of the electric field on the barrier height of the gate is considered. In this case, the range of electric field values at which

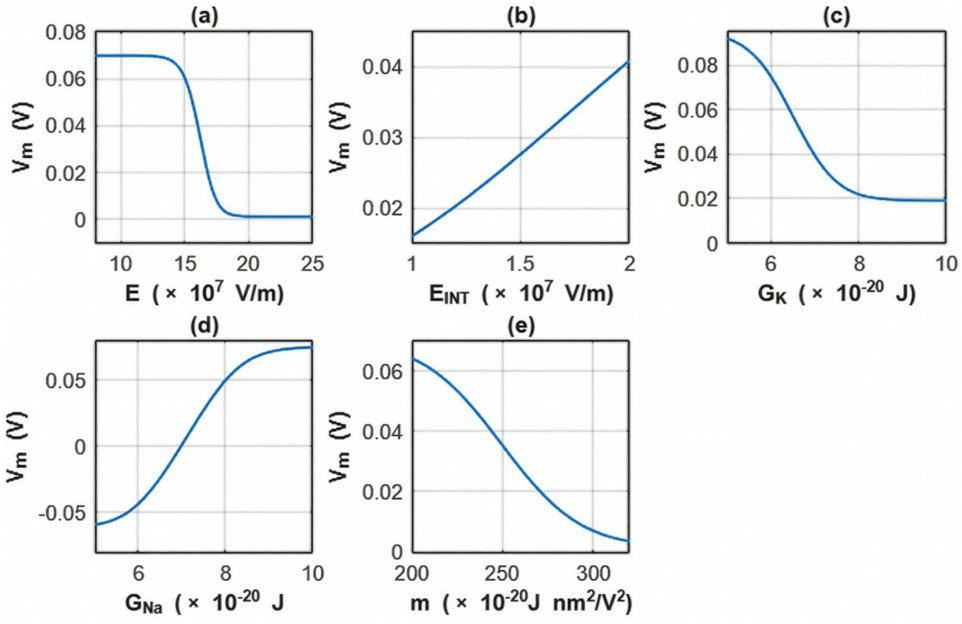

Figure 17 The changes in the membrane potential across the range of one parameter while holding other parameters constant at their average value for the fourth case. (**a**) the sensitivity analysis is done according to the range of the external electric field while holding other parameters constant at their average values. (**b**) The sensitivity analysis is done according to the range of the intrinsic electric field while holding other parameters constant at their average values. (**c**) the sensitivity analysis is done according to the range of the barrier height of potassium channel while holding other parameters constant at their average values. (**d**) the sensitivity analysis is done according to the range of the barrier height of sodium channel while holding other parameters constant at their average values. (**e**) The sensitivity analysis is done according to the range of the m value while holding other parameters constant at their average values.

https://doi.org/10.2147/JPR.S566042

depolarization occurs is $(3-8)\times 10^7$ V/m. On the other hand, hyperpolarization occurs when the direction of the external electric field is opposite to the direction of the internal electric field of the neuronal membrane as observed in Figures 10 and 11. The range of electric field values at which hyperpolarization up to 0.5 V occurs is $(11.5-22)\times 10^7$ V/m. On the other hand, according to Figure 12, the drop in the barrier height of the closed gates mediated by the electric fields can increase the number of open ion channels to permeate both sodium and potassium ions based on the Boltzmann distribution of thermal energy. In this case, a classical transport is prominent because open channels mean that the barrier height is lower than the kinetic energy of ions. This may indicate that quantum tunneling transport is more energetically favorable because the energy requirement is lower. The range of the required electric field to depolarize the membrane potential by the classical transport through open channels is generally within $(8-25)\times 10^7$ V/m.

Both approaches of investigation (the quantum and classical approaches) predict that electric fields generated by SCS can depolarize the membrane potential. However, when the parameters of potassium and sodium channels such as the barrier height of the hydrophobic gate G differ from each other, the classical approach fails to predict the stimulation effect mediated by SCS. When the barrier height of potassium K2P channels is lower than that of sodium NALCN channels, hyperpolarization is expected to occur instead of depolarization according to the classical transport, see Figure 13. This discrepancy is explained in the literature based on molecular structure of these channels and conductance values at the resting state of neurons. The molecular structure of NALCN channels reveals that the intracellular gate is sealed off by hydrophobic residues and by two other gates, while the intracellular gate of K2P channels is composed mainly by hydrophobic residues. Moreover, the resting conductance of potassium ions is 10–20 times higher than that of sodium ions. Such discrepancy in the values of the barrier height can hyperpolarize the membrane potential larger than 0.07 V, which decreases the excitability of neurons. Consequently, the proposed segmental and supra-segmental therapeutic effects of stimulating A-beta and descending fibers cannot exist. In this case, the quantum approach can explain the therapeutic effects of stimulation because quantum tunneling of potassium ions can depolarize the membrane potential regardless of the discrepancy in the values of barrier height between potassium and sodium channels. In the context of energetic requirement, we are referring to the energy needed to initiate or elicit the depolarization and not the energy required in restoring the electrical potential and the related metabolic processes such as upregulation proteins and signal transmission. So, if both models share the same energetic demand in terms of restoring the potential and the other metabolic costs, our study shows that the quantum model uses less energy to elicit the depolarization. This adds the advantage for the quantum model over the classical one and may reduce the energetic demand on the neuronal cells at least from this aspect. We compared the two models using the r values described in the results section. They are used to measure the average energy required to change the membrane potential by 0.01 V by using 1×10^7 V/m electric field. Close observation to the Tables 2–11, the r values for the quantum tunneling-assisted depolarization is between 4 to 30 times lower than the classical depolarization. This means quantum tunneling utilizes average energy less than the classical model by 4 to 30 times, which may give quantum tunneling the energetic advantage to occur over the classical transport. Moreover, given the mitochondrial dysfunction and the impairment in the energy production in the neurons of chronic neuropathic pain,[32–34] it seems that quantum tunneling can stimulate neurons without exacerbating the mitochondrial dysfunction by adding lower energetic burden on mitochondria. On the other hand, depolarization induced by classical transport may add larger energetic demand on mitochondria and worsen the mitochondrial dysfunction which in turn results in poor therapeutic outcome of SCS. Furthermore, the results showed that quantum tunneling can induce large membrane depolarization as the strength of the electric field increases. This large depolarization can be remarkable, dropping below 50 mV, which is represented in the previous figures. This can lead to depolarization blockade which arrests the initiation of action potentials, which in turn decreases the pain signals coming from the periphery to the brain centers. Eventually, this contributes to the analgesic effect made by SCS. Again, quantum tunneling guarantees the occurrence of such large depolarization regardless of the discrepancy between the barrier height values of potassium and sodium channels.

In the Table 16 below, a comparison between the quantum and classical model with regard to the pain modulation is shown. Based on this comparison in Table 16, clinical implications can be provided. Even though SCS is a reasonable alternative intervention when the pharmacological interventions fail to manage neuropathic pain, not all patients benefit

Table 16 A Comparison Between the Quantum and Classical Models

The quantum Model	The classical Model
It can explain depolarization when the barrier heights of sodium and potassium channels are the same.	It can explain depolarization only when the barrier heights of sodium and potassium channels are the same.
It can explain depolarization by SCS even when the barrier heights of potassium channels are lower than these for sodium channels	It can NOT explain depolarization when the barrier heights of potassium channels are lower than these of sodium channels
Hyperpolarization is expected by the model only if the influence of the electric field on the kinetic energy of ions is considered and when the external electric field is in opposite direction to the electric field of the neuronal membrane. Small and large depolarization can occur. Small depolarization refers to the depolarization that increases the excitability of neurons but not large enough to cause blockade. Large one is the depolarization that leads to block in signal transmission.	Hyperpolarization, small and large depolarizations are expected to occur.
If hyperpolarization occurs, it is much larger than that observed in the classical model. Hence, it is more likely to inhibit the neuronal electrical activity and to contribute to the analgesic effect of SCS.	Hyperpolarization is lower than that observed in the quantum model.
If the influence of the external electric field on the kinetic energy of ions is not considered, then across all the ranges of G, m and, E_{INT}, the range of electric field used to induce depolarization is between $(11.5-24)\times 10^7$ V/m, while the range is $(3-8)\times 10^7$ V/m when the influence of the external electric field on the kinetic energy of ions is considered along with its influence on the barrier height of the gate. Hence, the net range is $(3-24)\times 10^7$ V/m.	Across all the ranges of G, m and, E_{INT},the range of electric field used to induce depolarization is between $(8-25)\times 10^7$ V/m.
For the same values of m, G and E_{INT}, the range of the external electric field required for depolarization is narrower than that of the classical model.	For the same values of m, G and E_{INT}, the range of the external electric field required for depolarization is wider than that of the quantum model.
The quantum tunneling-assisted depolarization requires less average energy to change the potential. This may minimize the energetic burden on mitochondria.	The depolarization induced by opening ion channels requires more average energy to change the potential. This may increase the energetic burden on mitochondria.

from SCS and may not achieve satisfactory pain relief. Accordingly, the quantum approach suggests explanations for such nonresponse to SCS. If the classical behavior of ions is dominating, then the two explanations are: 1) failure to induce depolarization can weaken the analgesic effect of SCS due to the absence of the segmental and supra-segmental mechanisms which are dependent on frequent depolarizations. 2) even when depolarizations occur, the higher energetic demand posed on mitochondria may offset the therapeutic effects by depolarizations since overwhelming mitochondria result in more oxidative stress and more inflammation which may worsen the pathological processes underlying the chronic neuropathic pain. Therefore, if these quantum effects are proven to contribute significantly to the therapeutic mechanisms of SCS, then optimizing the techniques of SCS to overcome the limitations of the classical model would be an interesting research area. Quantum bioinformatics is an intriguing multidisciplinary field that helps researcher to develop, design and model computational tools and techniques by optimizing the quantum principles.[57] Therefore, experts in the field of quantum bioinformatics may optimize the SCS techniques so that they can sustain the quantum behavior of ions within ion channels in the biological environment, which is hot and noisy that may collapse the quantum waves of ions. By doing so, these modified techniques may guarantee the occurrence and maintenance of the quantum tunneling and thus taking the advantage of the depolarization with less energetic costs.

Even though the model is not yet experimentally validated, the values of physical parameters are chosen to fit the scale of ion channels, and the model showed reasonable flexibility, especially regarding the major implications of the study when the parameters of the model change. Our analysis in the results section involved a wide range of values

consistent with the physical plausibility reported in the references, including a range of the coupling factor m between $(200-320)\times10^{-20}$ J nm^2 V^{-2}, a range of E_{INT} between $(1-2)\times10^7$ V/m, and a range of barrier height G between $(5-10)\times10^{-20}$ J, and the two main conclusions of the study remain validated across these ranges. In addition, the ranges of external electric fields E of both the quantum and classical models were near each other as explained in Table 16. The two main conclusions are depolarization induced by quantum tunneling is expected to occur regardless of the discrepancy in the values of the barrier height between sodium and potassium channels and it requires less energy if it is compared with depolarization induced by opening the channels. Based on the sensitivity analysis in Tables 12–15 and Figures 14–17, the first case predicts depolarization in the membrane potential below 0.07 V and may fall below zero when the barrier height of sodium channels is lower than that of potassium channels with no observation of membrane potential above 0.07 V that leads to hyperpolarization. When the membrane potential falls below zero and becomes negative value, this means that it is positive inside the neuron with respect to outside, which is the reversed polarity of the resting state of the neuron. In the second case, depolarization is expected to occur below 0.07 V and may fall below zero both when the barrier height of sodium channels is lower than that of potassium channels and when the barrier height of potassium channels is lower than that of sodium channels, with no observation of membrane potential above 0.07 V that leads to hyperpolarization. In the third case, depolarization is not expected to occur but hyperpolarization above 0.07 V is predicted and may reach large values up to 1.3 V. In addition, another distinctive pattern is observed in this case, which is not present in other cases. The low sensitivity of the membrane potential is found to change in response to the changes in the barrier height of potassium and sodium channels. In the fourth case, depolarization is observed and may fall below zero only when the barrier height of sodium channel is lower than that of potassium channels, while hyperpolarization can be predicted only when the barrier height of potassium channels is lower than that of sodium channels. This hyperpolarization does not exceed 0.1 V, which is 10 times lower than the hyperpolarization predicted by the quantum model.

The quantum model predicted that SCS can depolarize or hyperpolarize the membrane potential. Interestingly, recent experimental studies conducted on mouse spinal cord and retinal ganglion cells showed the same pattern of membrane potential changes predicted by the quantum model providing empirical evidence on the validity of the model.[58,59] In addition, they argued that small to moderate depolarizations increase the neuronal excitability, while large depolarizations lead to suppression of the neuronal excitability.[58,59] Hyperpolarization was also observed and it can modulate the neuronal activity.[58,59] All of these electrical changes can contribute to the therapeutic mechanisms of SCS, which were consistently predicted by the quantum tunneling model. Moreover, there is a paradoxical observation has been reported in the literature that can support our model.[60,61] This observation is that the gain-of-function (GOF) mutations of potassium channels result in neuronal hyperexcitability and seizure,[60,61] which is a paradoxical outcome because this type of mutation means that the flux of potassium ions to outside the neurons increases, which results in hyperpolarization that represents a state of hypoexcitability. Several explanations have been proposed to solve this paradoxical effect which includes: 1) the hyperpolarization of inhibitory interneurons results in the disinhibition of excitatory neurons.[62] 2) the increase in the activity of potassium channels results in an increase in the repolarization phase of action potential and its frequency.[63] 3) hyperpolarization can result in depolarization indirectly via the activation of hyperpolarization-activated cationic currents.[64] In this context and in the context of SCS, the activation of potassium channels either by GOF mutations or by the electric fields of SCS decreases the energy cost for the permeation of potassium ions thus increasing the tunneling probability of extracellular potassium ions over intracellular ions because they have higher kinetic energy. As a consequence, an inward cationic current of potassium ions instead of an outward current is generated to depolarize the neuron's membrane potential. As a result, the quantum tunneling model can explain the stimulatory effects of SCS and the paradoxical effect of GOF mutations. Another biological phenomenon related to our results is paradoxical hypokalemic depolarization in which a decrease in extracellular potassium concentration results in membrane depolarization instead of hyperpolarization.[65] To explain this paradoxical outcome, they proposed that the drop in the concentration of extracellular potassium ions alter the selectivity of the selectivity filter of K2P channels enabling them to conduct inward sodium current which is responsible for the paradoxical depolarization. All the attempts to explain the paradoxical behavior of potassium channels are based on the classical rules of electrophysiology, and none of

the proposed mechanisms were able to attribute the depolarization effect to potassium ions directly. Therefore, in the next section, we will provide concrete experimental approaches that can be used to validate the role of potassium ions tunneling in the paradoxical depolarization and the role of quantum tunneling of ions in the function of ion channels and the stimulatory effects of SCS.

Up to the authors' knowledge, there is not yet concrete and direct experimental evidence on the tunneling of ions through the closed gates of channels but the theoretical and mathematical frameworks and assumptions do not pose any limitation for such type of transport to occur within ion channels. The reason behind the lack of experimental evidence is the difficulty of measuring the quantum tunneling behavior in a hot and noisy environment using classical methods such as single channel patch clamp experiments which result in collapsing the quantum waves of ions. In other words, the quantum wave behavior, which allows ions to tunnel, will be lost as a consequence of experimental measurement. Another reason is that the field of quantum biology of ion channels particularly at the level of the closed gate is still in the infancy stage. Hence, our research group tries to implement mathematical tools to reveal the potential of quantum mechanics of addressing important topics in the fields of medicine and biology and encourages researchers to come up with new measurement techniques that can capture the quantum wavy behavior of particles. Recently, a group of researchers developed what is called the THz-trapped ion model that enables them to investigate the quantum tunneling transport in the selectivity filter of ion channels[66] by using electromagnetic waves in the level of Terahertz to trap ions in the zero point energy. They concluded that quantum transport can achieve higher values of conductance with lower kinetic energy requirements for ions, which is similar to the conclusions that we report here in our study. Interestingly, two other proposed experimental methods including THz resonance fluorescence and the intense field non-resonant are suggested by the same authors to study the quantum tunneling transport. Other experimental methods that have the potential to measure the quantum tunneling of ions include Nitrogen-Vacancy (NV) centers and the patch-clamp amplifier.[67,68] Here, we will provide several concrete experimental approaches to validate the role of quantum tunneling and to distinguish it from the classical transport using the appropriately designed methods and technology to measure quantum tunneling:

1. One of the major distinguishing features of quantum model that is expected to observe is detecting an electric current through the closed gate which is not classically expected to conduct any current or permeate ions. In addition, by applying external electric field on ion channels, and detecting the tunneling current along with the applied voltage, the experimental findings should show a slope (I/V) as in the following equation:

$$\frac{I}{V} = \frac{q^2}{h} e^{-\frac{\sqrt{8\pi^2 M}}{\hbar} L\left(\sqrt{G - m(E - E_{INT})^2} - \sqrt{KE}\right)}, \tag{15}$$

Interestingly, this equation predicts certain feature that can be used to test the quantum model experimentally, which is the exponential dependence of the slope on the length of the closed gate, the mass of the ion, the barrier height of the gate, the coupling factor m, the external and the intrinsic electric fields, and the kinetic energy of the ion. If the experimental findings prove such a relationship, it will be supportive evidence on the role of quantum tunneling in the function of ion channels.

2. Another experimental approach to test the quantum model is to measure isotopic differences in the electrical current using the kinetic isotope effect (KIE). Potassium has two stable isotopes K^{39} and K^{41}. These two isotopes have different masses. So, experimental measurement may show a difference in the quantum electrical current between these two isotopes as in the following equation:

$$\frac{I_{K^{39}}}{I_{K^{41}}} = e^{\sqrt{M_{K^{41}}} - \sqrt{M_{K^{39}}} \left(\frac{\sqrt{8\pi^2}}{\hbar} L\left(\sqrt{G} - \sqrt{KE}\right)\right)}, \tag{16}$$

 https://doi.org/10.2147/JPR.S566042

Based on Equation (16), the tunneling current of the isotope 39 is larger than the current of the isotope 41 because as the mass of the particle increases, the tunneling probability decreases exponentially.

3. At physiological parameters, the quantum model predicts the ability of potassium ions to depolarize the membrane potential due to discrepancy between extracellular and intracellular potassium ions in terms of quantum conductance and tunneling current. As a consequence, experiments may show a ratio higher than one between the tunneling current of extracellular potassium ions and the tunneling current of intracellular potassium ions as in the following equation:

$$\frac{I_{ion_o}}{I_{ion_i}} = e^{\frac{\sqrt{8\pi^2 M}}{\hbar} L\left(\sqrt{KE_o} - \sqrt{KE_i}\right)}, \tag{17}$$

4. A more complex experimental approach is observing a depolarization in the membrane potential mediated via quantum tunneling, especially in the case in which the energy barrier of potassium channels is lower than that of sodium channels or where potassium channels are the dominant channels in the membrane, which is not predicted to occur under the rules of classical electrophysiology. In this approach, changing the residues of the closed gate of potassium channels to change their barrier height can provide further details on the relationship between the energy of the barrier, the tunneling current and the degree of membrane depolarization. Additionally, observing an inward tunneling current of potassium ions along with depolarized membrane potential provides evidence on the role of quantum tunneling in affecting the excitability of neurons. Moreover, utilizing different intensities of external electric field and applying it on potassium channels to alter their barrier height is another promising approach to investigate the quantum tunneling-induced depolarization of the membrane.

The present study predicts the values of electric field to be within the magnitude of 10^7 V/m to alter the neuronal membrane potential. However, up to authors' knowledge and based on the present literature, there is no reporting for the intensity of the electric field produced by SCS by experiments. Hence, our article is the first to predict the range of electric field values required for neuronal stimulation based on quantum and classical models. However, the values of electric field induced by SCS can be predicted and calculated based on the parameters of SCS using the following equation:

$$E = \frac{1}{4\pi\varepsilon_r\varepsilon_0} \cdot \frac{q}{r^2}, \tag{18}$$

where E is the electric field generated by electrical charges, ε_0 is the electrical permittivity of vacuum, ε_r is the relative permittivity of neuronal membrane, r is the distance between charges and neurons and q is the charge generated by SCS.

For r = 3–5 mm,[69,70] $\varepsilon_0 = 8.85 \times 10^{-12}$ F/m, $\varepsilon_r = 2 - 5$ for lipid bilayer neuronal membrane,[71] electrical current (I) values used by SCS equal to $(0.1 - 5)$ mA[72,73] and time (t) or pulse width equals to $50 - 500\mu s$,[72,74] the electric field calculated from these parameters can yield the obtained range of electric field stated in the study, which is within the magnitude of 10^7 V/m. The charges q generated by SCS can be calculated by the following equation $q = It$.

Our model focuses on ion channels involved in determining the resting membrane potential, and theoretically speaking every type of ion channel is a candidate for quantum tunneling. However, in the context of our study, there are certain requirements must be met in the type of ion channels to be included. First, these channels must be involved primarily in determining the resting membrane potential. Second, these channels must possess a hydrophobic gate so that the electric field can affect its energetics. For example, voltage-gated ion channels are an important type of ion channels that are involved in action potential initiation and propagation and some types have a hydrophobic gate. In this case, electric fields can affect the barrier height of their gates but whether this can affect the dynamics of the action potential or have any therapeutic effects in the context of SCS in neuropathic pain is a major research question that needs further analysis and investigation in future papers. In addition, a recent study investigated the tunneling time of potassium ions in G-quadruplex structures[75] and found that it was within the scale of picoseconds, which is a sufficiently short time to

induce depolarization and action potential. However, further investigation is required to explore the tunneling times of sodium and potassium ions in specific situations such as ion channels under the influence of external electric field.

Limitations

In this section, we would like to mention the limitations of our work so that they can be addressed in future works to increase the validity of the quantum tunneling model. First, detailed graphs for the mean potential forces should be obtained for the closed gates of K2P and NALCN channels so that the present conclusions can be replicated with greater credibility. Second, in vivo neurons are not uniformly aligned, and membrane orientations vary hence the angle between the electric field and the neuronal membrane might not be 0 or 180 degree. Therefore, exploring the conditions in which the angle is between 0 and 180 is necessary to validate the results to real biological environment. Third, our model requires experimental testing to verify the significance of quantum tunneling in ion channels and its role in determining the excitability of neurons and in the therapeutic mechanisms of SCS.

Conclusions

The quantum tunneling model predicts that depolarization between 0.07 V until 0 V induced by SCS occurs even when the barrier height of potassium channels is lower than that for sodium channels, unlike the classical model that fails to make such a predication. Furthermore, quantum tunneling-assisted depolarization induced by SCS utilizes less energy by 4 to 30 times compared with the classical model. However, providing experimental evidence on the significance of quantum tunneling in inducing depolarization by SCS is vital to add a greater validity to the quantum model. Therefore, we provided several experimental approaches that are reasonable and feasible and can be used to test the quantum tunneling model.

Use of AI Tools Declaration

The authors declare they have not used Artificial Intelligence (AI) tools in the creation of this article.

Institutional Review Board Statement

Not applicable because the study is computational with mathematical modelling, hence no participants or patients were recruited.

Data Sharing Statement

Data and MATLAB codes are available upon a reasonable request from the corresponding author.

Author Contributions

All authors made a significant contribution to the work reported, whether that is in the conception, study design, execution, acquisition of data, analysis and interpretation, or in all these areas; took part in drafting, revising or critically reviewing the article; gave final approval of the version to be published; have agreed on the journal to which the article has been submitted; and agree to be accountable for all aspects of the work.

Funding

This research received no external funding.

Disclosure

The authors declare no conflicts of interest in this work.

References

1. Attal N, Bouhassira D, Colvin L. Advances and challenges in neuropathic pain: a narrative review and future directions. *Br J Anaesth*. 2023;131(1):79–92. doi:10.1016/j.bja.2023.04.021
2. Apkarian AV, Baliki MN, Geha PY. Towards a theory of chronic pain. *Prog Neurobiol*. 2009;87(2):81–97. doi:10.1016/j.pneurobio.2008.09.018

3. Baron R, Binder A, Wasner G. Neuropathic pain: diagnosis, pathophysiological mechanisms, and treatment. *Lancet Neurol*. 2010;9(8):807–819. doi:10.1016/S1474-4422(10)70143-5
4. Themistocleous AC, Backonja MM. Pathophysiology of Neuropathic Pain. In: *Diabetic Neuropathy: Advances in Pathophysiology and Clinical Management*. Cham: Springer International Publishing;2023:415–425. doi:10.1007/978-3-031-15613-7_23
5. Cui CX, Liu HY, Yue N, Du YR, Che LM, Yu JS. Research progress on the mechanism of chronic neuropathic pain. *IBRO Neurosci Rep*. 2023;14:80–85. doi:10.1016/j.ibneur.2022.12.007
6. Smith PA. Neuropathic pain; what we know and what we should do about it. *Front Pain Res*. 2023;4. doi:10.3389/fpain.2023.1220034.
7. Thouaye M, Yalcin I. Neuropathic pain: from actual pharmacological treatments to new therapeutic horizons. *Pharmacol Ther*. 2023;251:108546. doi:10.1016/j.pharmthera.2023.108546
8. Xie W, Strong JA, Meij JT, Zhang JM, Yu L. Neuropathic pain: early spontaneous afferent activity is the trigger. *Pain*. 2005;116(3):243–256. doi:10.1016/j.pain.2005.04.017
9. Djouhri L, Koutsikou S, Fang X, McMullan S, Lawson SN. Spontaneous pain, both neuropathic and inflammatory, is related to frequency of spontaneous firing in intact C-fiber nociceptors. *J Neurosci*. 2006;26(4):1281–1292. doi:10.1523/JNEUROSCI.3388-05.2006
10. Petroianu GA, Aloum L, Adem A. Neuropathic pain: mechanisms and therapeutic strategies. *Front Cell Develop Biol*. 2023;11:1072629. doi:10.3389/fcell.2023.1072629
11. Asmedi A, Wibowo S, Meliala L. Ephaptic crosstalk in painful diabetic neuropathy: an electrodiagnostic study. *J Med Sci*. 2018;50:173–179. doi:10.19106/JMedSci005002201806
12. Seltzer Z, Devor M. Ephaptic transmission in chronically damaged peripheral nerves. *Neurology*. 1979;29(7):1061. doi:10.1212/WNL.29.7.1061
13. Morris CE. Voltage-gated channel mechanosensitivity: fact or friction? *Front Physiol*. 2011;2:25. doi:10.3389/fphys.2011.00025
14. Amir R, Argoff CE, Bennett GJ, et al. The role of sodium channels in chronic inflammatory and neuropathic pain. *J Pain*. 2006;7(5):S1–29. doi:10.1016/j.jpain.2006.01.444
15. Levinson SR, Luo S, Henry MA. The role of sodium channels in chronic pain. *Muscle Nerve*. 2012;46(2):155–165. doi:10.1002/mus.23314
16. Finnerup NB, Kuner R, Jensen TS. Neuropathic pain: from mechanisms to treatment. *Physiol Rev*. 2020;101(1):259–301. doi:10.1152/physrev.00045.2019
17. Sun L, Peng C, Joosten E, et al. Spinal cord stimulation and treatment of peripheral or central neuropathic pain: mechanisms and clinical application. *Neural Plast*. 2021;2021(1):5607898. doi:10.1155/2021/5607898
18. Ferraro MC, Gibson W, Rice AS, Vase L, Coyle D, O'Connell NE. Spinal cord stimulation for chronic pain. *Lancet Neurol*. 2022;21(5):405. doi:10.1016/S1474-4422(22)00096-5
19. Bianconi S, Leppik L, Oppermann E, Marzi I, Henrich D. Direct Current Electrical Stimulation Shifts THP-1-Derived Macrophage Polarization towards Pro-Regenerative M2 Phenotype. *Int J Mol Sci*. 2024;25(13):7272. doi:10.3390/ijms25137272
20. Li C, Levin M, Kaplan D. Bioelectric modulation of macrophage polarization. *Sci Rep*. 2016;6(21044). doi:10.1038/srep21044
21. Nawafleh S, Qaswal AB, Alali O, et al. Quantum mechanical aspects in the pathophysiology of neuropathic pain. *Brain Sciences*. 2022;12(5):658. doi:10.3390/brainsci12050658
22. Kim Y, Bertagna F, D'souza EM, et al. Quantum biology: an update and perspective. *Quantum Rep*. 2021;3(1):80–126. doi:10.3390/quantum3010006
23. Hameroff S. 'Orch OR'is the most complete, and most easily falsifiable theory of consciousness. *Cognitive Neurosci*. 2021;12(2):74–76. doi:10.1080/17588928.2020.1839037
24. Georgiev DD, Glazebrook JF. The quantum physics of synaptic communication via the SNARE protein complex. *Prog Biophys Mol Biol*. 2018;135:16–29. doi:10.1016/j.pbiomolbio.2018.01.006
25. Griffiths DJ, Schroeter DF. *Introduction to Quantum Mechanics*. Cambridge university press; 2018 Aug 16.
26. Nakajima T, Delbecq MR, Otsuka T, et al. Coherent transfer of electron spin correlations assisted by dephasing noise. *Nat Commun*. 2018;9(1):2133. doi:10.1038/s41467-018-04544-7
27. Rebentrost P, Mohseni M, Kassal I, Lloyd S, Aspuru-Guzik A. Environment-assisted quantum transport. *New J Phys*. 2009;11(3):033003. doi:10.1088/1367-2630/11/3/033003
28. Hameroff S, Penrose R. Consciousness in the universe: a review of the 'Orch OR'theory. *Phys Life Revi*. 2014;11(1):39–78. doi:10.1016/j.plrev.2013.08.002
29. Cao J, Cogdell RJ, Coker DF, et al. Quantum biology revisited. *Sci Adv*. 2020;6(14):eaaz4888. doi:10.1126/sciadv.aaz4888
30. Breuer HP, Laine EM, Piilo J, Vacchini B. Colloquium: non-Markovian dynamics in open quantum systems. *Rev Mod Phys*. 2016;88(2):021002. doi:10.1103/RevModPhys.88.021002
31. Jedlicka P. Revisiting the quantum brain hypothesis: toward quantum (neuro) biology? *Front Mol Neurosci*. 2017;10:366. doi:10.3389/fnmol.2017.00366
32. Li DY, Liu L, Liu DQ, Zhang LQ, Zhou YQ, Mei W. Mitochondrial calcium overload contributes to mechanical allodynia in neuropathic pain via inducing mitochondrial dynamic imbalance. *Int Immunopharmacol*. 2025;158:114863. doi:10.1016/j.intimp.2025.114863
33. Ribeiro PS, Willemen HL, Eijkelkamp N. Mitochondria and sensory processing in inflammatory and neuropathic pain. *Front Pain Res*. 2022;3:1013577. doi:10.3389/fpain.2022.1013577.
34. Doyle TM, Salvemini D. Mini-Review: mitochondrial dysfunction and chemotherapy-induced neuropathic pain. *Neurosci lett*. 2021;760:136087. doi:10.1016/j.neulet.2021.136087
35. Li XY, Toyoda H. Role of leak potassium channels in pain signaling. *Brain Res Bull*. 2015;119:73–79. doi:10.1016/j.brainresbull.2015.08.007
36. Huang L, Xu G, Jiang R, Luo Y, Zuo Y, Liu J. Development of non-opioid analgesics targeting two-pore domain potassium channels. *Curr Neuropharmacol*. 2022;20(1):16. doi:10.2174/1570159X19666210407152528
37. Mathie A, Veale EL. Two-pore domain potassium channels: potential therapeutic targets for the treatment of pain. *Pflügers Archiv-Euro J Physiol*. 2015;467(5):931–943. doi:10.1007/s00424-014-1655-3
38. Zhang D, Wei Y. Role of sodium leak channel (NALCN) in sensation and pain: an overview. *Front Pharmacol*. 2024;14:1349438. doi:10.3389/fphar.2023.1349438
39. Qaswal AB. Quantum tunneling of ions through the closed voltage-gated channels of the biological membrane: a mathematical model and implications. *Quantum Rep*. 2019;1(2):219–225. doi:10.3390/quantum1020019

40. Qaswal AB, Ababneh O, Khreesha L, Al-Ani A, Suleihat A, Abbad M. Mathematical modeling of ion quantum tunneling reveals novel properties of voltage-gated channels and quantum aspects of their pathophysiology in excitability-related disorders. *Pathophysiology*. 2021;28(1):116–154. doi:10.3390/pathophysiology28010010
41. Aryal P, Sansom MS, Tucker SJ. Hydrophobic gating in ion channels. *J Mol Biol*. 2015;427(1):121–130. doi:10.1016/j.jmb.2014.07.030
42. Yazdani M, Jia Z, Chen J. Hydrophobic dewetting in gating and regulation of transmembrane protein ion channels. *J Chem Phys*. 2020;153(11). doi:10.1063/5.0017537
43. Rao S, Klesse G, Lynch CI, Tucker SJ, Sansom MS. Molecular simulations of hydrophobic gating of pentameric ligand gated ion channels: insights into water and ions. *J Phys Chem B*. 2021;125(4):981–994. doi:10.1021/acs.jpcb.0c09285
44. Aryal P, Abd-Wahab F, Bucci G, Sansom MS, Tucker SJ. A hydrophobic barrier deep within the inner pore of the TWIK-1 K2P potassium channel. *Nat Commun*. 2014;5(1):4377. doi:10.1038/ncomms5377
45. Mathie A, Al-Moubarak E, Veale EL. SYMPOSIUM REVIEW: gating of two pore domain potassium channels. *J Physiol*. 2010;588 (17):3149–3156. doi:10.1113/jphysiol.2010.192344
46. Xie J, Ke M, Xu L, et al. Structure of the human sodium leak channel NALCN in complex with FAM155A. *Nat Commun*. 2020;11(1):5831. doi:10.1038/s41467-020-19667-z
47. Khavrutskii IV, Gorfe AA, Lu B, McCammon JA. Free energy for the permeation of Na+ and Cl− ions and their ion-pair through a zwitterionic dimyristoyl phosphatidylcholine lipid bilayer by umbrella integration with harmonic Fourier beads. *J Am Chem Soc*. 2009;131(5):1706–1716. doi:10.1021/ja8081704
48. Eckart C. The penetration of a potential barrier by electrons. *Physical Review*. 1930;35(11):1303. doi:10.1103/PhysRev.35.1303
49. Chandra AK. *Introductory Quantum Chemistry*. 4 Edn ed. McGraw-Hill; 1974.
50. Serway RA, Moses CJ, Moyer CA. *Modern Physics*. 2004.
51. Klesse G, Tucker SJ, Sansom MS. Electric field induced wetting of a hydrophobic gate in a model nanopore based on the 5-HT3 receptor channel. *ACS nano*. 2020;14(8):10480–10491. doi:10.1021/acsnano.0c04387
52. Lohrasebi A, Sajadi M. Effect of external electric fields on the potential energy profile of K+ ions in selective filter of the KcsA potassium channel. *Mol Simulat*. 2014;40(13):1067–1073. doi:10.1080/08927022.2013.840905
53. Han Y, Wu L, Jiao T, Gao Q. Effect of an Electric Field on Surface Properties of Hydrophobic Particles during a Flotation Process in Salt Water. *Langmuir*. 2020;36(30):8922–8928. doi:10.1021/acs.langmuir.0c01376
54. Huang J, Chen J. Hydrophobic gating in bundle-crossing ion channels: a case study of TRPV4. *Biophys J*. 2023;122(3):109a. doi:10.1016/j.bpj.2022.11.770
55. Hall JE, Hall ME. *Guyton and Hall Textbook of Medical Physiology E-Book: Guyton and Hall Textbook of Medical Physiology E-Book*. Elsevier Health Sciences; 2020 Jun 13.
56. Qaswal AB. Quantum electrochemical equilibrium: quantum version of the Goldman–Hodgkin–Katz equation. *Quantum Rep*. 2020;2(2):266–277. doi:10.3390/quantum2020017
57. Mokhtari M, Khoshbakht S, Ziyaei K, Akbari ME, Moravveji SS. New classifications for quantum bioinformatics: q-bioinformatics, QCt-bioinformatics, QCg-bioinformatics, and QCr-bioinformatics. *Briefings Bioinf*. 2024;25(2):bbae074. doi:10.1093/bib/bbae074
58. Karnup S, Daugherty S, Tai C, Yoshimura N. Response of dorsal horn neurons in mice to high-frequency (kHz) biphasic stimulation is not sensitive to local temperature rise. *Physiological Reports*. 2025;13(3):e70205. doi:10.14814/phy2.70205
59. Lee JI, Werginz P, Kameneva T, Im M, Fried SI. Membrane depolarization mediates both the inhibition of neural activity and cell-type-differences in response to high-frequency stimulation. *Commun Biol*. 2024;7(1):734. doi:10.1038/s42003-024-06359-3
60. Niday Z, Tzingounis AV. Potassium channel gain of function in epilepsy: an unresolved paradox. *Neuroscientist*. 2018;24(4):368–380. doi:10.1177/1073858418763752
61. Nappi P, Miceli F, Soldovieri MV, Ambrosino P, Barrese V, Taglialatela M. Epileptic channelopathies caused by neuronal Kv7 (KCNQ) channel dysfunction. *Pflügers Archiv-Euro J Physiol*. 2020;472(7):881–898. doi:10.1007/s00424-020-02404-2
62. Miceli F, Soldovieri MV, Ambrosino P, et al. Early-onset epileptic encephalopathy caused by gain-of-function mutations in the voltage sensor of Kv7. 2 and Kv7. 3 potassium channel subunits. *J Neurosci*. 2015;35(9):3782–3793. doi:10.1523/JNEUROSCI.4423-14.2015
63. Du W, Bautista JF, Yang H, et al. Calcium-sensitive potassium channelopathy in human epilepsy and paroxysmal movement disorder. *Nature Genet*. 2005;37(7):733–738. doi:10.1038/ng1585
64. Robinson RB, Siegelbaum SA. Hyperpolarization-activated cation currents: from molecules to physiological function. *Ann Rev Physiol*. 2003;65 (1):453–480. doi:10.1146/annurev.physiol.65.092101.142734
65. Jurkat-Rott K, Weber MA, Fauler M, et al. K+-dependent paradoxical membrane depolarization and Na+ overload, major and reversible contributors to weakness by ion channel leaks. *Proc Natl Acad Sci*. 2009;106(10):4036–4041. doi:10.1073/pnas.0811277106
66. Wang K, Wang S, Yang L, Wu Z, Zeng B, Gong Y. THz trapped ion model and THz spectroscopy detection of potassium channels. *Nano Res*. 2021;1–9. doi:10.1007/s12274-021-3965-z
67. Hall LT, Hill CD, Cole JH, et al. Monitoring ion-channel function in real time through quantum decoherence. *Proc Natl Acad Sci*. 2010;107 (44):18777–18782. doi:10.1073/pnas.1002562107
68. Jiang T, Yi L, Liu X, Ivanov AP, Edel JB, Tang L. Fabrication of electron tunneling probes for measuring single-protein conductance. *Nature Protocols*. 2023;18(8):2579–2599. doi:10.1038/s41596-023-00846-3
69. Harland B, Kow CY, Svirskis D. Spinal intradural electrodes: opportunities, challenges and translation to the clinic. *Neural Regenerat Res*. 2024;19 (3):503–504. doi:10.4103/1673-5374.380895
70. Zander HJ, Graham RD, Anaya CJ, Lempka SF. Anatomical and technical factors affecting the neural response to epidural spinal cord stimulation. *J Neural Engi*. 2020;17(3):036019. doi:10.1088/1741-2552/ab8fc4
71. Gramse G, Dols-Pérez A, Edwards MA, Fumagalli L, Gomila G. Nanoscale measurement of the dielectric constant of supported lipid bilayers in aqueous solutions with electrostatic force microscopy. *Biophys J*. 2013;104(6):1257–1262. doi:10.1016/j.bpj.2013.02.011
72. Gmel GE, Santos Escapa R, Parker JL, Mugan D, Al-Kaisy A, Palmisani S. The effect of spinal cord stimulation frequency on the neural response and perceived sensation in patients with chronic pain. *Front Neurosci*. 2021;15:625835. doi:10.3389/fnins.2021.625835
73. Joosten EA, Franken G. Spinal cord stimulation in chronic neuropathic pain: mechanisms of action, new locations, new paradigms. *Pain*. 2020;161 (Supplement 1):S104–13. doi:10.1097/j.pain.0000000000001854

74. Yearwood TL, Hershey B, Bradley K, Lee D. Pulse width programming in spinal cord stimulation: a clinical study. *Pain Physician*. 2010;13(4):321. doi:10.36076/ppj.2010/13/321
75. Celebi Torabfam GK, Demir G, Demir D. Quantum tunneling time delay investigation of K+ ion in human telomeric G-quadruplex systems. *J Biol Inorg Chem*. 2023;28(2):213–224. doi:10.1007/s00775-022-01982-z